NAVAL POSTGRADUATE SCHOOL

MONTEREY, CALIFORNIA

THESIS

ORGANIC MARITIME ISAR EFFICACY VIA AROMA DATA ALGORITHM

by

Fernando M. Lenis

June 2023

Thesis Advisor: David A. Garren
Second Reader: Ric Romero

THIS PAGE INTENTIONALLY LEFT BLANK

REPORT DOCUMENTATION PAGE	*Form Approved OMB No. 0704-0188*

1. AGENCY USE ONLY *(Leave blank)*	**2. REPORT DATE** June 2023	**3. REPORT TYPE AND DATES COVERED** Master's thesis

4. TITLE AND SUBTITLE
ORGANIC MARITIME ISAR EFFICACY VIA AROMA DATA ALGORITHM

5. FUNDING NUMBERS

6. AUTHOR(S) Fernando M. Lenis

7. PERFORMING ORGANIZATION NAME(S) AND ADDRESS(ES)
Naval Postgraduate School
Monterey, CA 93943-5000

8. PERFORMING ORGANIZATION REPORT NUMBER

9. SPONSORING / MONITORING AGENCY NAME(S) AND ADDRESS(ES)
N/A

10. SPONSORING / MONITORING AGENCY REPORT NUMBER

11. SUPPLEMENTARY NOTES The views expressed in this thesis are those of the author and do not reflect the official policy or position of the Department of Defense or the U.S. Government.

12a. DISTRIBUTION / AVAILABILITY STATEMENT
Approved for public release. Distribution is unlimited.

12b. DISTRIBUTION CODE
A

13. ABSTRACT (maximum 200 words)

Synthetic aperture radar (SAR) is an invaluable part of the overarching information, surveillance, and reconnaissance (ISR) architecture. Traditional SAR elements, particularly aircraft and satellites, are detached from the consumers of SAR imagery. SAR imagery as a product is produced via the relative motion between the radar and the scattering centers of the target of interest. Thus, simulation is conducted to determine whether it is possible to develop a SAR system that can be used for imagery on the consumer level. Arbitrary rigid object motion autofocus (AROMA) simulates the pitch and roll of a surface vessel by way of a physical signal model designed to include both translational and rotational motion. AROMA uses this method to mitigate phase errors induced by target motion and generate images as though the target remained stationary, lending significant utility for maritime target identification. The validity of AROMA as a means of imagery production is evaluated through simulation of a SAR system with AROMA as an image processer, against a target experiencing varying sea state conditions.

14. SUBJECT TERMS
information, surveillance, and reconnaissance, ISAR, arbitrary rigid object motion autofocus, AROMA, maximum likelihood, target detection, synthetic aperture radar, SAR

15. NUMBER OF PAGES
71

16. PRICE CODE

17. SECURITY CLASSIFICATION OF REPORT	**18. SECURITY CLASSIFICATION OF THIS PAGE**	**19. SECURITY CLASSIFICATION OF ABSTRACT**	**20. LIMITATION OF ABSTRACT**
Unclassified	Unclassified	Unclassified	UU

NSN 7540-01-280-5500

Standard Form 298 (Rev. 2-89)
Prescribed by ANSI Std. 239-18

THIS PAGE INTENTIONALLY LEFT BLANK

Approved for public release. Distribution is unlimited.

ORGANIC MARITIME ISAR EFFICACY VIA AROMA DATA ALGORITHM

Fernando M. Lenis
Lieutenant, United States Navy
BS, Florida Agricultural and Mechanical University, 2016

Submitted in partial fulfillment of the
requirements for the degree of

MASTER OF SCIENCE IN ELECTRICAL ENGINEERING

from the

NAVAL POSTGRADUATE SCHOOL
June 2023

Approved by: David A. Garren
Advisor

Ric Romero
Second Reader

Douglas J. Fouts
Chair, Department of Electrical and Computer Engineering

THIS PAGE INTENTIONALLY LEFT BLANK

ABSTRACT

Synthetic aperture radar (SAR) is an invaluable part of the overarching information, surveillance, and reconnaissance (ISR) architecture. Traditional SAR elements, particularly aircraft and satellites, are detached from the consumers of SAR imagery. SAR imagery as a product is produced via the relative motion between the radar and the scattering centers of the target of interest. Thus, simulation is conducted to determine whether it is possible to develop a SAR system that can be used for imagery on the consumer level. Arbitrary rigid object motion autofocus (AROMA) simulates the pitch and roll of a surface vessel by way of a physical signal model designed to include both translational and rotational motion. AROMA uses this method to mitigate phase errors induced by target motion and generate images as though the target remained stationary, lending significant utility for maritime target identification. The validity of AROMA as a means of imagery production is evaluated through simulation of a SAR system with AROMA as an image processer, against a target experiencing varying sea state conditions.

THIS PAGE INTENTIONALLY LEFT BLANK

TABLE OF CONTENTS

THIS PAGE INTENTIONALLY LEFT BLANK

LIST OF FIGURES

THIS PAGE INTENTIONALLY LEFT BLANK

LIST OF ACRONYMS AND ABBREVIATIONS

AROMA	arbitrary rigid object motion autofocus
DTE	detect-to-engage
DB	decibel
EHF	extremely high frequency
ELF	extremely low frequency
EM	electromagnetic
IC	Intelligence Community
ISR	Intelligence Surveillance and Reconnaissance
MATLAB	Matrix Laboratory
NEETS	Navy Electricity and Electronics Training Series
PPR	pre-planned responses
RADAR	radio detection and ranging
RCS	radar cross section
SAR	synthetic aperture radar
SHF	super high frequency
SIR	signal-to-interference ratio
SNR	signal-to-noise ratio

THIS PAGE INTENTIONALLY LEFT BLANK

I. INTRODUCTION

Intelligence, surveillance, and reconnaissance (ISR) systems used by the intelligence community (IC) provide decision makers and warfighters the ability to determine the capabilities, patterns of life, and orientation of possible threats with high fidelity. However, the landscape of current ISR systems is far removed from the platforms and combatants that rely on this information to identify targets and develop firing solutions. In naval warfighting doctrine, particularly in the fire control and weapons systems disciplines, the concept of the detect-to-engage (DTE) sequence is considered a cornerstone of successful threat mitigation: the shorter the time from detection to engagement, the more likely it is for a platform to successfully neutralize any threat within an area of operation. The faster and more accurate the detection part of this sequence can be conducted, directly translates to a higher probability of defeating threats. Current pre-planned responses (PPR), that include the DTE sequence, rely heavily upon organic systems, (i.e., radar), to identify targets due to the immediate collection and interpretation of information. Immediate identification and warning of threats are the main mission of the intelligence community and are essential in ensuring the proper targets are identified and, when necessary, are neutralized.

Without the use of ISR, the amount of information available to a naval surface combatant is limited primarily to location, heading, and speed as determined via several radar systems and on-board processing. However, with the leveraging of ISR, the information available to decision makers is robust. Overhead imagery satellites are a key part in assessing possible threats, and while they are not readily available as a controllable resource to the average surface combatant, overhead imagery is a decision-making advantage, nonetheless. However, due to the nature of the orbits within which these satellites operate, these assets are limited to specific targets over specific periods of time to manage competing intelligence requirements. In that respect, the surface combatant is left mostly without access to these types of tools for decision making and will only be given the product of these systems in a time delayed fashion.

There is a need to provide as much information to surface combatants as quickly as possible. To do so, this research seeks to answer whether a system can be developed to deliver this type of information to the surface combatants more rapidly and be under the control of those individuals who would be responding to threats in the DTE sequence. Currently, the fastest way to do so is to use maritime patrol and reconnaissance aircraft that will fly different missions to gather different types of intelligence, not limited to but including, imagery. However, this method of imagery collection comes at a cost and is usually not within the control of an individual surface combatant. This project will investigate whether a SAR imagery capability onboard a surface vessel is a viable option, and will do so in varying sea state conditions.

II. BACKGROUND

This chapter establishes the foundational knowledge necessary to understand the operation of synthetic aperture radar (SAR). The phenomenon of reflection, refraction, and diffraction are defined as likely scenarios of what ultimately occurs when any radar is operated, including SAR. Next, this chapter discusses the interactions between radio waves and the environment. The radar range equation (RRE) is introduced as an extension of understanding the propagation of radio waves as specifically applied to the transmission and receipt of radar emissions. Once a working knowledge of the RRE is established, this chapter then discusses the basic geometry and operating modes of SAR as well as the process in which SAR and inverse synthetic aperture radar (ISAR) imagery is formed. Furthermore, the mechanics of how the AROMA code mimics the motion of the ocean as it affects the roll, pitch, and yaw of a vessel via a power law random process are discussed.

A. RADAR FUNDAMENTALS

As an advanced application of a radar, SAR is an asset that allows for higher fidelity of target and threat recognition for decision makers and warfighters. SAR at its core develops images using wideband echoes at different positions through relative movement between the target and the collector [1]. To understand SAR, a deep understanding of radar fundamentals is necessary.

Radar, as a means of understanding an operational environment and possible threat layout, is an essential aspect of military operations. As described in *Principles of Modern radar* Volume 1, radar is an electrically driven system that uses the radio frequency part of the electromagnetic (EM) spectrum to transmit radio waves towards an intended target or environment, and in doing so, a radar can fulfill three fundamental functions: find targets, track targets, and in the case of SAR, develop imagery [2]. Once these waves are transmitted, the reflection of these waves against targets is collected via a receiver and processed to a display that conveys whether there is a positive return or negative return. Radars can operate across the entire radio frequency part of the EM spectrum from ELF (0--300 Hz) to EHF (30--300 GHZ). [2]

In the radio frequency portion of the EM spectrum, the emissions that are transmitted are fundamentally the same as other parts of the spectrum and are simply just waves of energy. This energy is characterized by an electric field and magnetic field orthogonal to each other moving in the direction of propagation as the wave moves through free space [3]. Based upon the frequency, these waves can be classified as ground waves, space waves, or sky waves susceptible to three types of disturbances: reflection, refraction, diffraction [3]. For the purposes of this discussion, disturbances will be attributed to an individual classification of waves for simplicity.

Of these disturbances that radio waves experience, reflection is the fundamental disturbance that allows for a radar to detect a signal return from an unknown object for follow on processing such as developing imagery. Reflection is the process by which an EM wave interacts with a dense environment and returns energy back towards the transmitter. In the EM wave propagation through the atmosphere, reflection happens most commonly in the ionosphere, 50–400 miles above the surface of the Earth [3]. The ionosphere is made up of charged particles that interact with ultraviolet radiation from the sun whereby the electrons in the outer shell of these particles are excited to a higher energy state in a process known as excitation. The excitation of charged particles makes the ionosphere denser and increases the rate of reflection EM waves encounter. Although there is not a singular start and end point to the range of frequencies that are affected by ionospheric reflection, this phenomenon usually affects medium frequency to low very high frequency waves [3]. Although all waves are susceptible to reflection, in radio wave propagation sky waves are normally the bulk of observable points of this type of interaction [3].

While reflection is an essential part of the operation of radar, when a radar transmits a signal through a medium this signal is not transmitted solely in a straight line. Reflection primarily occurs when the ionosphere contains more charged particles. However, when these charged particles are no longer experiencing excitation due to the solar UV rays, refraction is more likely to occur. Refraction is when a wave bends through a medium that has a different density than the originating medium [3]. This phenomenon is governed by Snell's law, which states that when there is a difference in the density of two medias, a

wave propagating through one medium to another will have an incident angle and refracted angle proportional to each other via the sine trigonometric function as seen in Figure 1. As a wave propagates through differing layers of the atmosphere with differing densities and indexes of refraction, the wave will bend. The main effect of this phenomenon is that it is possible to extend radio wave transmissions farther than they would normally be capable of and is commonly exploited for long range high frequency communications [3].

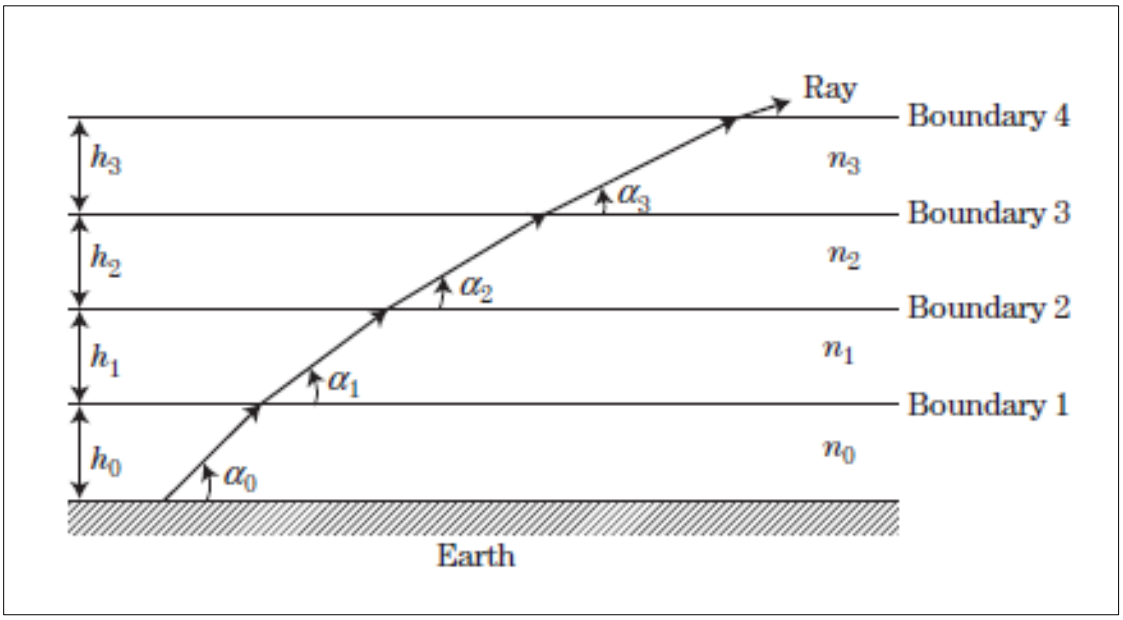

Figure 1. Path of a ray through a horizontally stratified atmosphere. Source: [2, Fig. 4–11].

Where refraction is the bending of waves in different media, which affects the travel of a radar return, diffraction is also seen as a bending of waves that affects both the transmission and return of radar emissions. Diffraction is when a wave curves around the edges of obstacles and can even spread into areas considered shadow zones where there is a complete absence of these waves in [2]. Diffraction happens most commonly with lower frequencies that propagate as ground waves as they interact with large physical obstructions similar in size to their wavelength [3]. This phenomenon is depicted in Figure 2 and Figure 3.

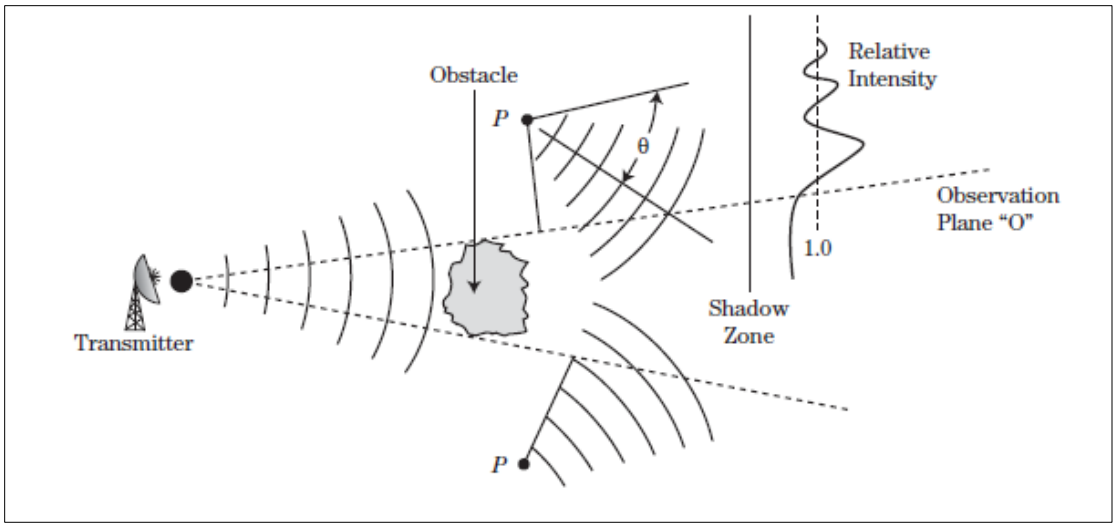

Figure 2. Illustration of virtual sources for diffraction around an obstacle. Source: [2, Fig. 4–24].

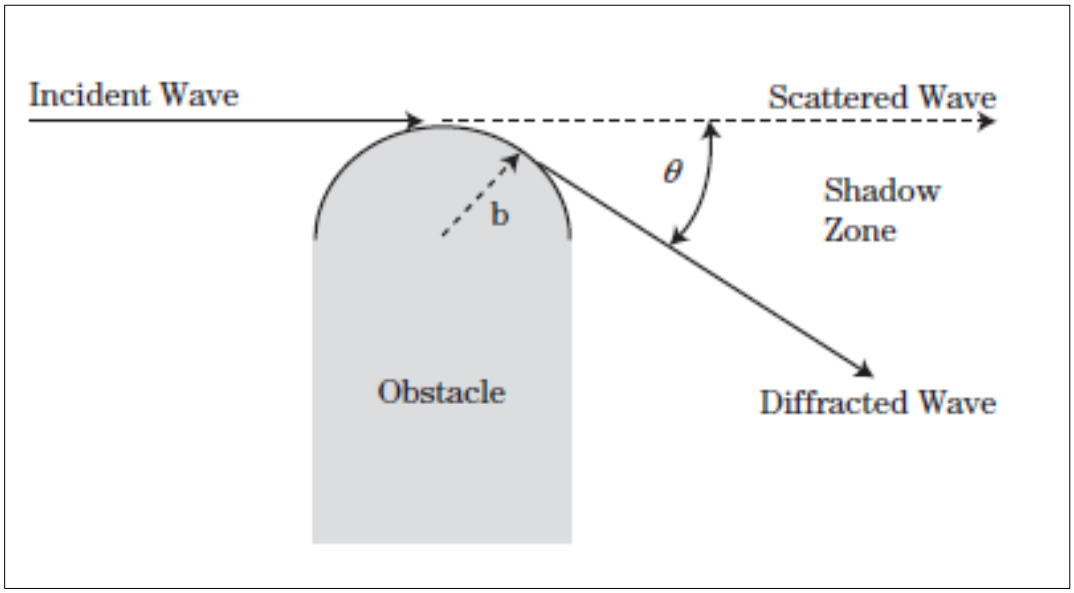

Figure 3. Geometry for diffraction into shadow zones. Source: [2, Fig. 4–25].

B. RADAR RANGE EQUATION

Although the function may be different, all radars are governed by the same laws of physics, and ultimately the same fundamental equation. The equation governing the ability of a radar to detect a target is the radar range equation (RRE), which describes the

signal to interference ratio (SIR) [2] of the radar. The SIR is the ratio of the total target signal power over all interfering signal power, and this value is more commonly written as the signal to noise ratio (SNR), as seen in the following equation from [2] where SNR is defined as

$$SNR = \frac{P_t G_t G_r \lambda^2 \sigma n_p}{(4\pi)^3 R^4 k T_0 F B L_s} \quad , \tag{1.1}$$

where

SNR = Signal to Noise Ratio,
P_t = Power of the Transmitter,
G_t = Gain of the Transmitter,
G_r= Gain of the Receiver,
λ = Wavelength of the transmitted signal,
σ= radar cross section of the target,
n_p= Number of pulses coherently combined,
R = One way Range between radar and target,
k = Boltzmann Constant,
T_0 = Standard Temperature,
F = Noise Figure,
B = Bandwidth of the signal,
L_s = Total losses.

C. SAR GEOMETRY

A radar used for finding and tracking can be most easily described in two dimensions from platform to target. In the case of SAR, there is more geometry involved to develop images with enough resolution to be usable. Resolution in this case refers to coherently processed received signals to develop a usable image for human interpretation. Thus, the higher the resolution, the clearer the image [1].

1. Azimuth and Range Resolution

Jiaguo Lu of the East China Research Institute of Electronic Engineering in the 2019 publication *"Design Technology of Synthetic Aperture Radar"* discusses the two-dimensional image resolution of a target in terms of range and azimuth resolution [1].

Range resolution can be thought of as the distance between two clearly identifiable points along an arbitrary horizontal axis, as a function of the difference in the arrival times of a leading edge and trailing edge of pulse echo [1]. Range resolution is governed by Equation 1.2

$$\Delta R_g = \frac{\Delta R_s}{\sin(\eta)} = \frac{c\tau_p}{2\sin(\eta)} \quad , \tag{1.2}$$

where

ΔR_g = range resolution, ground
ΔR_s = range resolution, slant
c = light speed
η = incident angle between the antenna and the ground
t_p = signal pulse width

and where the relationship between the speed of light, signal pulse width, and angle between the transmitter and a horizontal axis is used. An image of this relationship is represented in Figure 4.

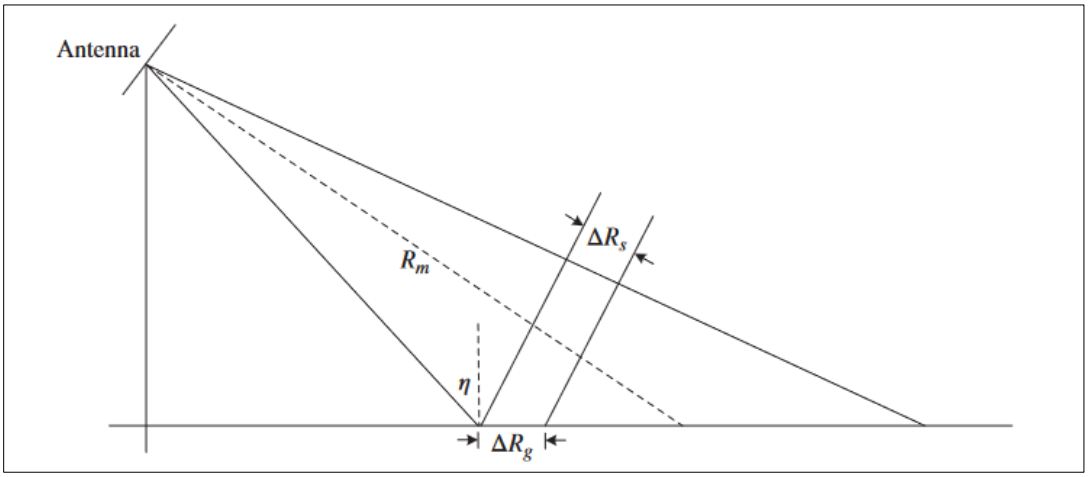

Figure 4. Sketch of range resolution geometry. Source: [1, Fig. 1.1].

While range resolution is a function of the distance between two points, in the case of defining azimuth resolution, the fundamental quality of SAR is due to relative motion between the two targets [1]. Exploitation of this motion leads to the formation of a virtual

antenna array, where the physical antenna is essentially replicated to increase the field of effect of the propagated wave. When this phenomenon occurs, the leading and trailing edges of the pulse echoes discussed in the definition of range resolution are stacked together in phase, and compression in the azimuth direction is performed to allow for high resolution, as seen in Figure 5. As a collection platform moves, the radar transmissions illuminate a greater area as though the aperture of the radar were larger. Thus, the azimuth resolution can be thought of as a measure of the fidelity of the resolution caused by what the new synthetic array is able to detect and process, it is described in [1] by Equation 1.3

$$R_{az} = \theta_s R = \frac{\lambda R}{2L_s} = \frac{\lambda R}{2} \cdot \frac{D}{\lambda R} = \frac{D}{2}, \tag{1.3}$$

where

θ_s= Equivalent Bandwidth of the Synthetic Aperture
R = Range
λ = Wavelength
L_s = Length of the Synthetic Aperture
D = The size of the antenna in the azimuth direction.

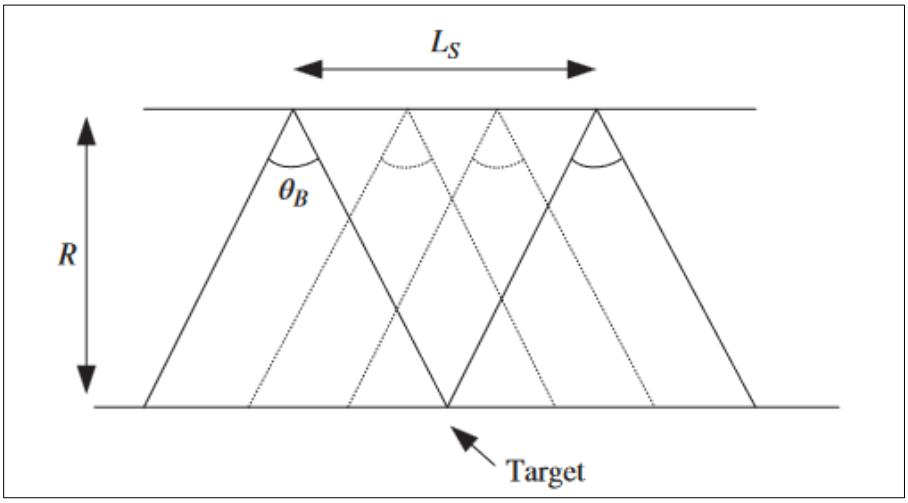

Figure 5. Diagram of synthetic aperture. Source: [1, Fig. 1.2].

2. Slant Range vs. Ground Range vs. Cross Range

As part of the discussion of azimuthal and range resolution, the concept of slant and cross range are important in understanding the function of SAR. Professor David Garren in [4] defines slant range as "the distance from the antenna of the collection platform to the center of the intended collection target." This means from the point in 3D space that the antenna is located, to the center of the target. The ground range is similar in definition to range resolution and is the range purely across the ground from the collector to the target [4]. The slant and ground range are related as depicted in Figure 6, where the relationship between the two is a geometric approach. The cross range is heavily used for the purposes of imaging and is the range orthogonal to the range direction and lies within the ground plane.

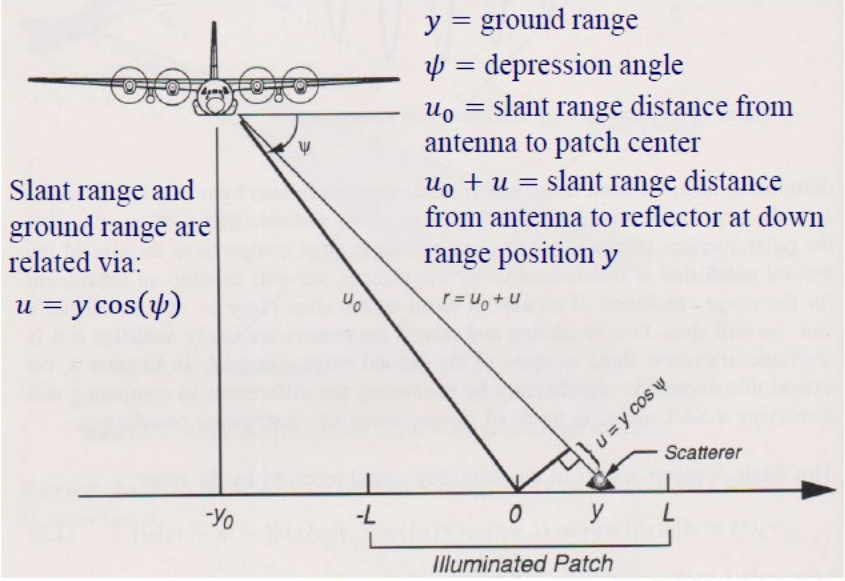

Figure 6. SAR collection geometry. Source: [4, Fig. 4].

D. SAR GEOMETRY

Due to different mission requirements that may arise, different modes of operation for SAR are necessary to obtain images that match the necessary specific requirements. Three common modes of operation to achieve these goals are strip map, spotlight, and scan.

1. Strip Map

As J. Lu discusses in the *Design Technology of Synthetic Aperture Radar*, the standard and simplest mode of SAR operation is strip map mode, which uses a fixed antenna that is pointed toward the ground so that the beam from it draws a "strip" on the ground as the collector moves [1]. The size of the imaged target is related to the size of the ground footprint of the radiation pattern of the radar, and the limiting factor in this mode is the time between transmissions of two consecutive pulses, also known as the pulse repetition interval (PRI) [1]. A schematic of this mode of operation is provided in Figure 7.

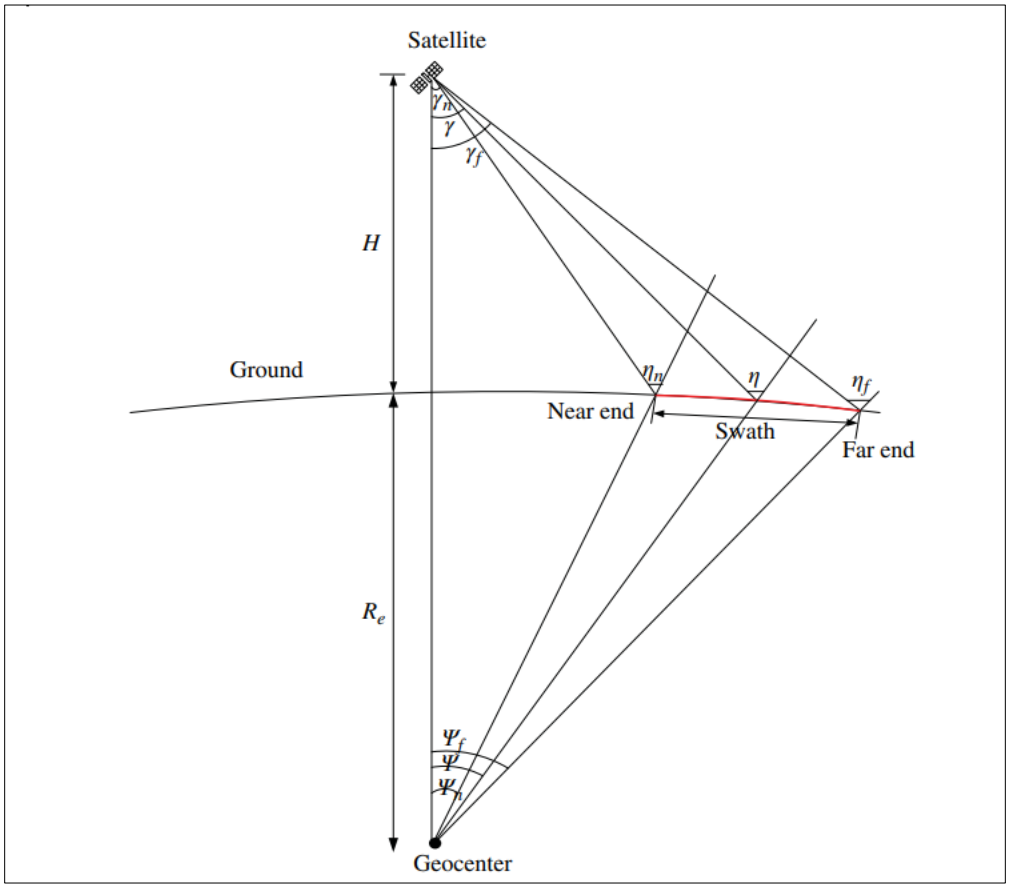

Figure 7. Schematic diagram of strip map SAR. Source: [1, Fig. 2.2].

2. Scan SAR

Scan mode in the context of SAR is used to ensure that a wide area can be imaged. In this mode of operation, the transmitter initially transmits a pulse and receives the return, repositions, and does the same process again in a different area [1]. The strip that is formed by the imaging and repositioning of the SAR allows for different parallel areas to be scanned, and a wider area is shown in the processed image [1]. The limiting quality of this mode of SAR is the decrease in azimuth resolution, and the requirement that the radar system be able to scan multiple areas quickly [1].

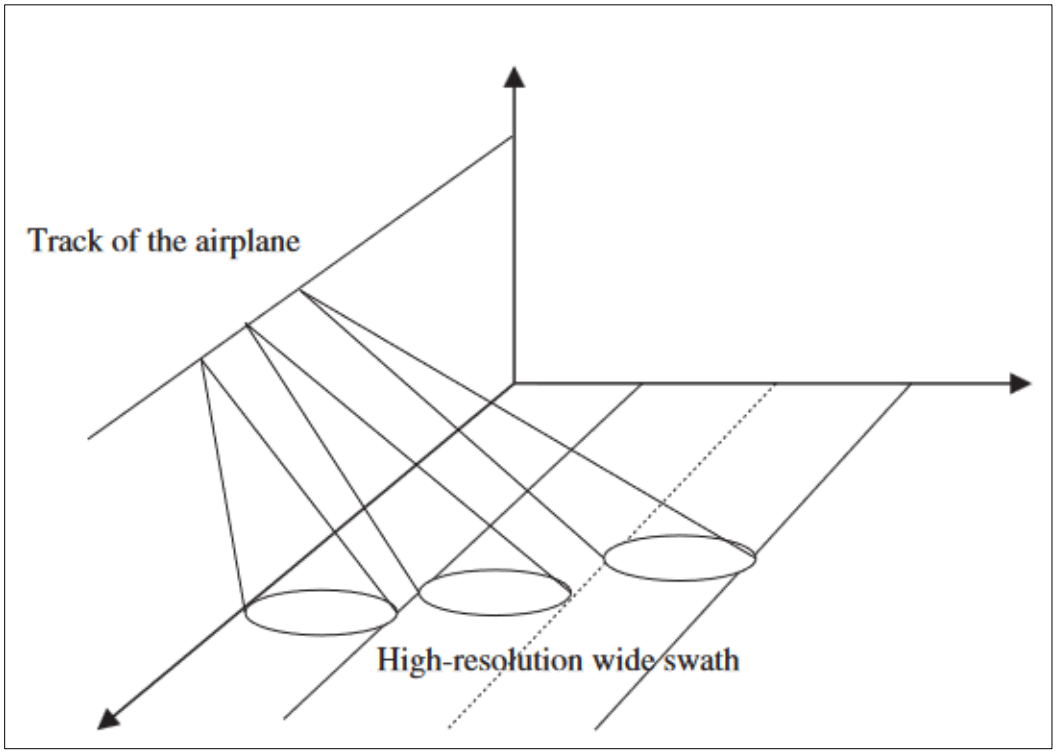

Figure 8. Diagram of scan SAR mode. Source: [1, Fig. 2.6].

3. Spotlight SAR

Spotlight SAR mode is specifically used for imaging a small area with very high resolution [1]. The increased resolution in both the range and azimuth domains is achieved by creating a synthetic aperture and focusing on a small target region for an extended period [1]. In a spotlight mode of operation, the collection platform maintains a straight-line path

and steady speed while the antenna array is pointed directly at the target [2]. A significant limit on the performance of the spotlight mode of operation occurs during situations where a longer collection period may be needed to image a specific target. The increased collection period then comes at the risk of erroneous returns from other regions along the specific flight path that may not contribute to a quality image of the target [2].

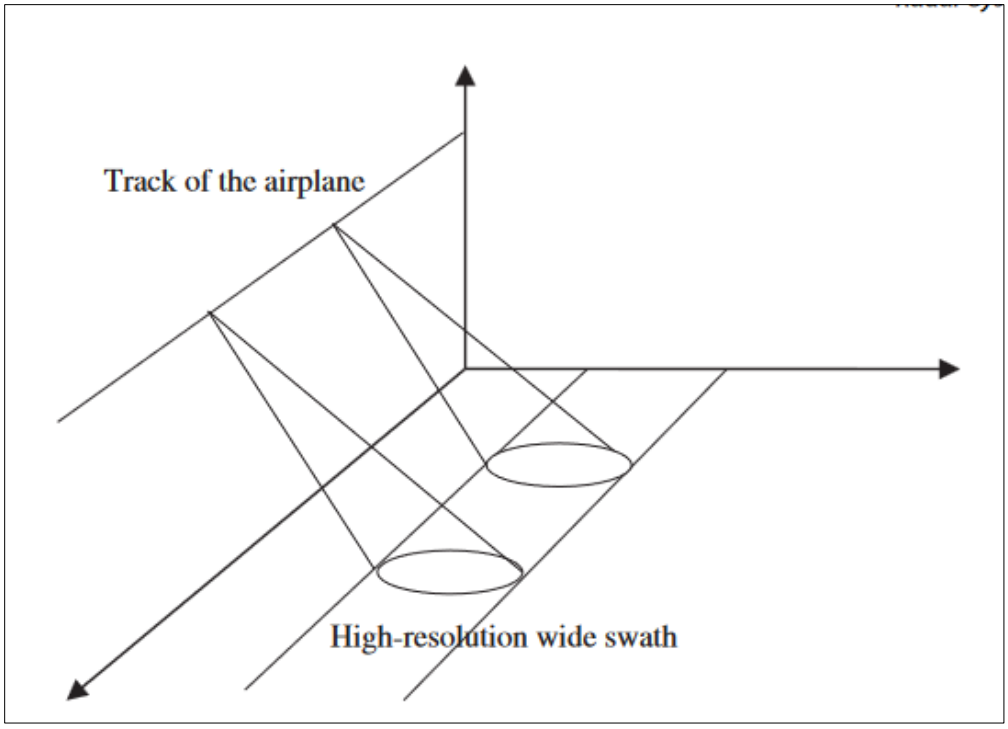

Figure 9. Diagram of spotlight SAR mode. Source: [1, Fig. 2.4].

E. SAR/ISAR IMAGERY FORMATION

Chen and Martorella discuss the fundamentals of ISAR imagery formation in their work *"Inverse Synthetic Aperture Radar Imaging: Principles, Algorithms and Applications,"* which will be used to lead the discussion in understanding how images are formed from SAR and ISAR platforms [5]. The fundamental difference between SAR and ISAR is the motion of the collector and target. In a SAR collection scenario, the motion of the radar antenna as it collects against a target is what produces the synthetic aperture. In the ISAR case, the roles are reversed such that target motion relative to the collector is

what causes the synthetic aperture. As will be discussed later in Chapter III, this thesis uses a scenario where both the collection platform and targeted platform are moving. However, the effects of the sea state do not affect the collection platform and therefore this scenario will be considered as an ISAR imagery scenario for the sake of discussion.

1. Doppler Effect

The first concept to introduce present in the formation of ISAR imagery is the Doppler effect [5]. The Doppler effect occurs when a radar transmits a signal towards a moving target, which causes the frequency of the received signal to be shifted from the frequency of transmission [5]. This shift in frequency is measured primarily in the frequency domain by taking the Fourier transform of the signal [5]. This allows for the shift in frequency to be easily identified via a view of the peaks and valleys present on a frequency domain graph commonly referred to as a Fourier spectrum plot. As mentioned in [5], the peak in the Fourier spectrum indicates the frequency shift that is caused by the velocity of the target movement, and for there to be accurate tracking of the target from the collecting radar transmitter, the transmitter must be driven by a highly stable source to assure that the received signal will be processed coherently.

The Doppler frequency shift [5] can be expressed in terms of the transmitter frequency, the target velocity with respect to the radar, and the speed of light as

$$f_D(t) = -f\left[\frac{2v(t)}{c}\right], \tag{1.4}$$

where

- f_D = Doppler Frequency Shift
- f = Carrier Frequency
- $v(t)$ = Target Velocity
- c = Speed of Light.

As it relates to the formation of imagery, the frequency shift caused by the Doppler effect from the relative motion of the target creates an image referred to as the motion induced image [5].

F. SIMULATED MOTION

As a means of developing SAR images, this thesis uses MATLAB code to simulate the motion of a surface vessel caused by varying sea states using a power law random process. These sea states are categorized numerically and will be discussed further. However, the effects specifically studied for the purposes of developing imagery are the roll, pitch, and yaw caused by these sea states.

1. Power Law Random Process and Phase Error

In [8] Garren discusses the methodology used to create arbitrary motion within the AROMA code. Based upon the works of Jakowatz in [9] and [10], AROMA uses a power law pseudorandom process to simulate the movement of a rigid target, which in the case of this thesis is modeled after a military naval vessel. Specifically in AROMA, the code is written to induce complicated non-linear rotational and translational motion to produce appropriate SAR smears for image formation [8]. AROMA then applies a physical signal model of both the rotation angles and the distances between points arising from the motion between the target and imaging radar [8].

Jakowatz discusses in [10] that the image formed from SAR imaging is produced as a function of the phase errors. These phase errors according to Jakowatz are typically modeled as power law random processes, whose characteristic function has a spectral density in the form of a decaying exponential [10]. While a discussion of the working mechanism of the power law random process is better served in a mathematics context, the application comes into play with this thesis in the sense that high frequency phase error functions are modeled closely using a power law process [10]. Figures 10 and 11 provide a physical view in the Fourier domain as to what the power law phase errors produce in an image, as compared to the impulse response of the image. In Figure 10, the simulated phase error for an image following a power-law spectral characteristic is provided as a function of aperture position, effective range, and phase error in radians. In Figure 11, the dashed line represents the impulse response for the image degraded by the power law phase error function of Figure 10. The solid line is the impulse response of the original image without phase errors.

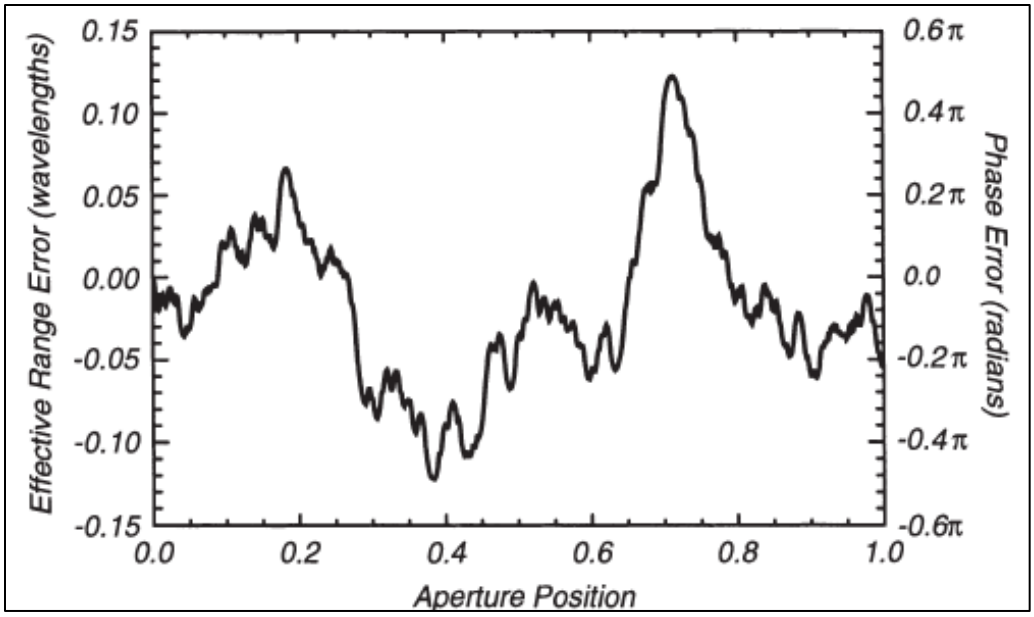

Figure 10. Simulated phase error with power-law spectral characteristics. Source: [10, Fig. 4.10].

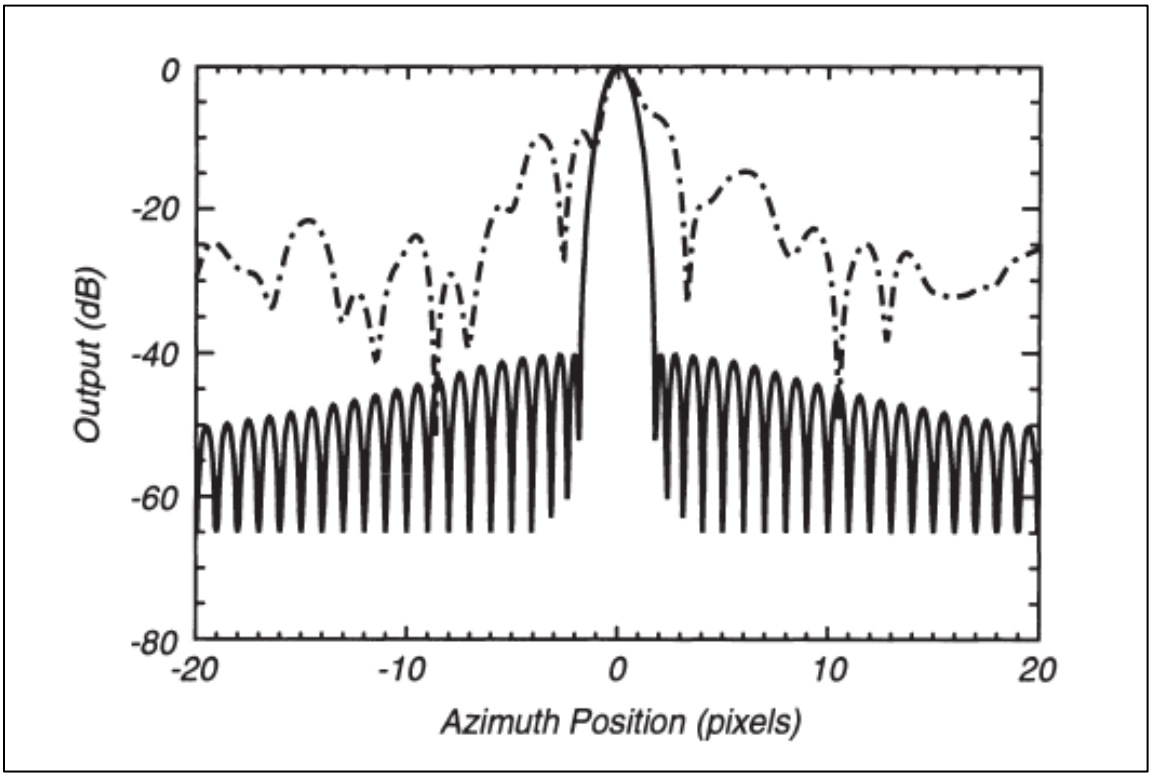

Figure 11. Diagram of impulse response vs. power law phase error function. Source: [10, Fig. 4.11].

2. Sea State Conditions

The final component for simulating motion properly is to understand the effects that the conditions of the ocean have upon a surface vessel. The state of the ocean is commonly referred to as sea states, with the National Weather Service providing a numerical designator to varying conditions [11]. Common operating conditions separate from operating in a storm are nominally around sea state 4 and below, as it is in the best interest of operational vessels to avoid operating in more perilous conditions for both structural and personnel safety.

THIS PAGE LEFT INTENTIONALLY BLANK

III. DESIGN METHODOLOGY

Chapter III discusses the approach to answering the research question "is it possible to develop a SAR system that can be used for imagery on board U.S. naval vessels?" To do so, this chapter discusses two phases of the experiment used to build a framework of what a SAR imagery system for U.S. naval vessels could be. The first phase used the AROMA code to simulate two surface combatants moving across a sea state condition that provided zero roll, pitch, or yaw angles on the target. The second phase used the AROMA code to develop this collection situation further by investigating the effects on imaging caused by the roll, pitch, and yaw angles from sea state 0 to sea state 4.

A. IMAGE FORMATION IN CALM SEAS

The initial phase of this experiment primarily consisted of the scenario set up for the second portion of the experiment. Prior to discussion of the initial parameters set, for the sake of experimentation there are certain factors of developing and simulating a potential SAR/ISAR capability that are not studied in this thesis. First, there is no discussion about the possible physical characteristics of this system to include antenna type, antenna size, and possible power consumption. Additionally, this experiment assumes a cooperative electromagnetic environment, and does not take into consideration any specific modulation schemes for transmission and receipt. Changes in frequency, target placement, and background clutter are also not discussed within this experiment. This experiment is focused solely on the efficacy of this capability being able to exist and not a measure of how to make performance improvements.

1. Target Development

The target used in this case was modeled after a standard U.S. naval vessel, with equidistant scattering centers. The scattering centers were fed into a three-dimensional matrix with varying intensities to mimic the size and orientation of a surface vessel. The target was placed at a down range of 50m and cross range of 100m from the collector. In Figure 13, the overhead view of the simulated vessel is shown, with the collection of

scattering centers in the center representing the mast of the vessel. The vessel in question is modeled after the shape and size of an average U.S. naval surface combatant.

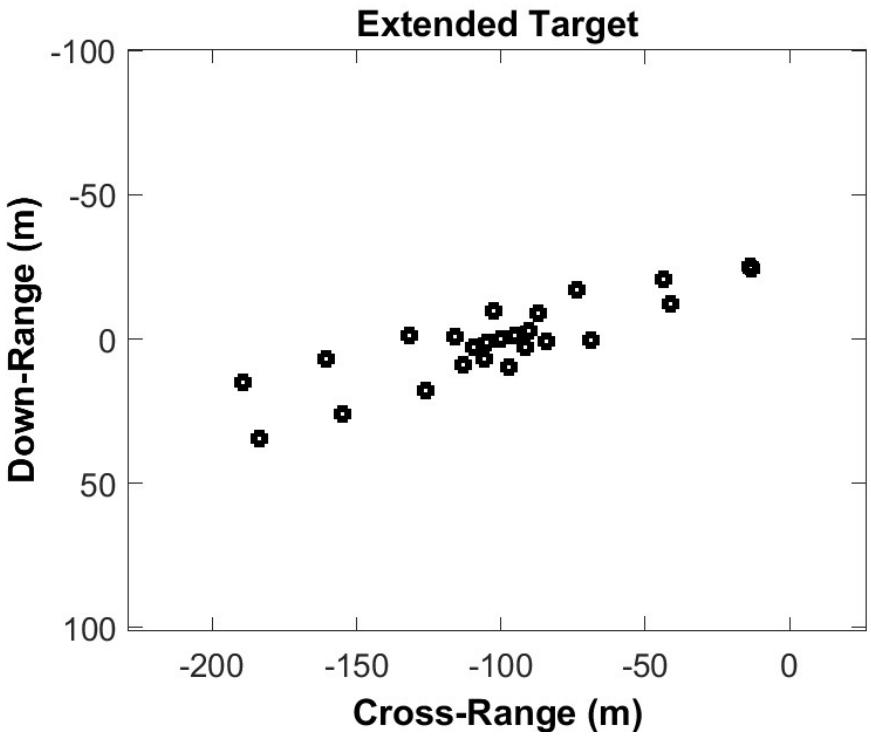

Figure 12. Simulated target scattering centers in the form of a surface vessel.

2. Sensor Parameters

The sensor parameters used for this experiment were chosen to give the sensor as close to a realistic design as possible and are provided in Table 1.

Table 1. Sensor Parameters.

Sensor Propagation Center Frequency	16.8 GHZ
Collection Platform Speed	15 m/s (~30 kts)
Propagation Ground Mid-Range	3000 m
Sensor Elevation	30 m
Elevation Angle	0 deg
Squint Angle	0 deg
Direction of Propagation	Right
Bandwidth	1.6 GHZ
Number of Frequency Samples	2000
Time duration	8 sec
Number of Waveforms	8000

The choice of the frequency to be 16.8 GHZ is such that any images produced will be high fidelity, as well as protected from possible electromagnetic interference due to the protected nature of EHF transmissions. Additionally, the choice of the speed of the collection platform, and sensor height, are in line with typical vessel speeds and mast heights from operational experiences.

3. SAR Images in Calm Seas

The use of the phrase “calm seas” as it relates to the development of SAR images for the purposes of this thesis will consist of the formation of a SAR image in sea state 0. The assumption for this phase of the experiment is that there is no change to the roll, pitch, or yaw in the formation of the image.

B. IMAGE FORMATION IN VARYING SEA STATES

Using the standards provided in [11], several assumptions were made to delineate different sea states based on the roll and pitch angles. First, there was a central peak to the sea state waves on the roll and pitch. Second, as discussed in Armin W. Dorry's *"Ship Dynamics for Maritime ISAR Imaging,"* there are design specifications with which the U.S. Navy designs their ships to [12]. Dorry states that typical pitch angles for sea state 4 are between one and two degrees, and roll angles are in the single digits in sea state 4 and below [12]. However, these values are not clearly attributed to the type of ship, therefore surveys of anecdotal experiences were collected from peers of the researcher, and ranges of angles were determined for roll and pitch based on sea states. Table 2 delineates the roll and pitch angles from sea states 0 to 4 that were used for this thesis.

Table 2. Roll and Pitch Angles for Sea States 0 to 4.

Sea State	**Roll Angle**	**Pitch Angle**
0	<1 Degree	<2 Degrees
1	<2 Degrees	<4 Degrees
2	<5 Degrees	<10 Degrees
3	<10 Degrees	<20 Degrees
4	<20 Degrees	<30 Degrees

IV. EXPERIMENTAL RESULTS

Chapter IV discusses the experimental results of the two phases of experimentation. In the first phase of results, the output of the AROMA code SAR imagery against the simulated target in sea state 0 is provided. In the second phase of results, the simulated target was given a roll and pitch analogous to varying sea conditions. The AROMA software is then applied to the images produced in phase two, to investigate the proficiency of the refocusing algorithm and its possible proficiency in operational use.

A. PHASE ONE—IMAGE FORMATION CALM SEAS (SEA STATE 0)

Image formation in calm seas produces the clearest results in image formation as expected. In Figure 14, the target yaw angle is represented. Due to yaw in the context of ship motion being the rotation about a central axis, the yaw angle is directly related to the ship heading in the results. As represented in Figures 15 and 16, the magnitude of the pitch and roll angles are minimal which in turn do not affect the output of the SAR image in an appreciable way. In Figure 15, using the power law pseudorandom process, the target roll due to the sea state was developed in a way that provides maximum roll angles of 2 degrees in line with the sea state determinations discussed previously. In Figure 16, the same is done for pitch. Figure 17 shows the default image created with no roll and pitch, and subsequently Figure 18 shows the difference when there is a slight roll and pitch angle still within the sea state 0 bounds to serve as a benchmark for image quality.

An aggregate representation of iterations one, five, ten, and fifteen of the AROMA image refocusing process is shown in Figure 19. As expected, in the later iterations of the AROMA process the image sharpness increases and the scattering centers are more clearly defined. The linear phase terms μ, ν, and ζ are represented in Figures 20, 21, and 22, respectively. As described in [8] μ is the linear phase term that gives a cross range shift varying with ground down range, ν is the linear phase term that measures the warping effect with respect to the ground cross range, and ζ is the linear phase term that is responsible for an offset in the cross range of the refocused image. These terms are represented across four iterations of the AROMA image refocusing processes. In each case, as the number of

refocusing iterations increases, the estimated value of these terms approaches the real value of the shifts as measured from the simulated target produced image. As the magnitude of the roll and pitch angles in sea state 0 are nearly zero, the linear phase shifts therefore are easily trackable. Due to yaw being directly related to the heading of the target, the representation of yaw depicted in Figure 14 will serve as the default for further imagery runs.

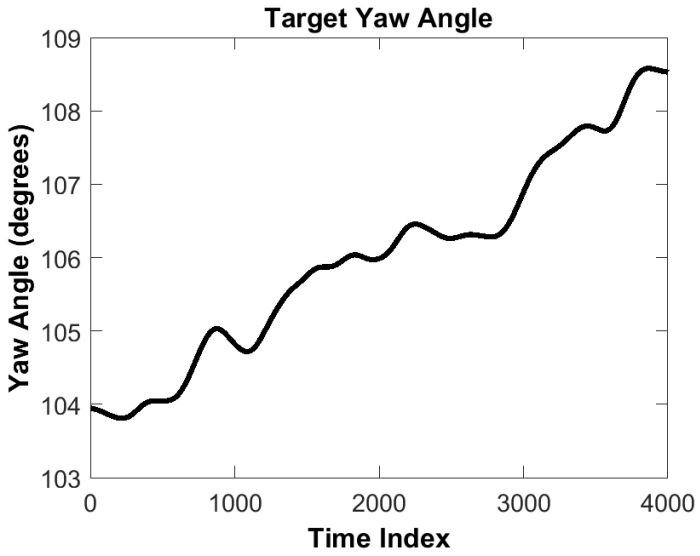

Figure 13. Sea state 0 yaw.

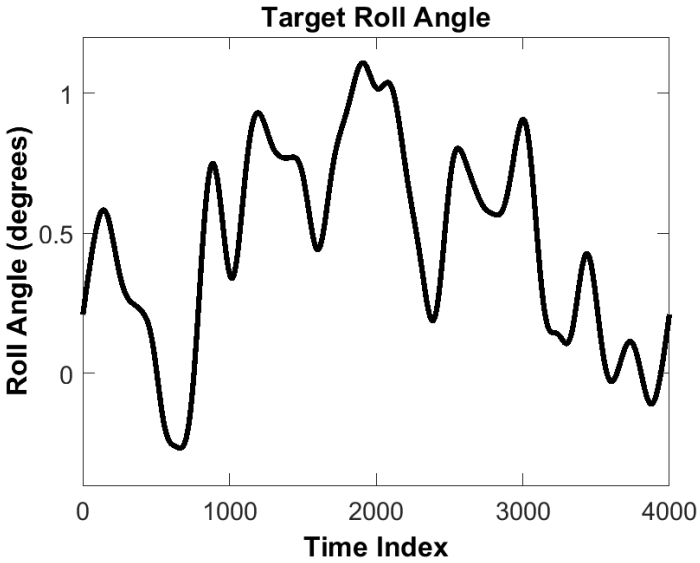

Figure 14. Sea state 0 roll angle.

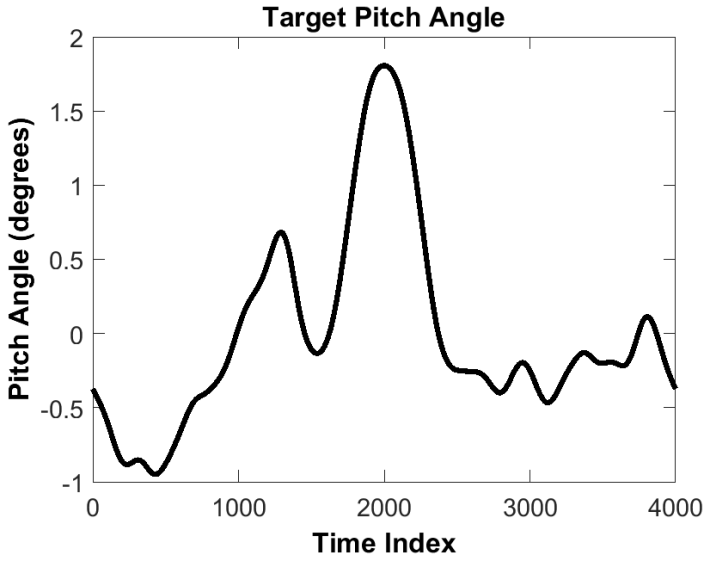

Figure 15. Sea state 0 pitch angle.

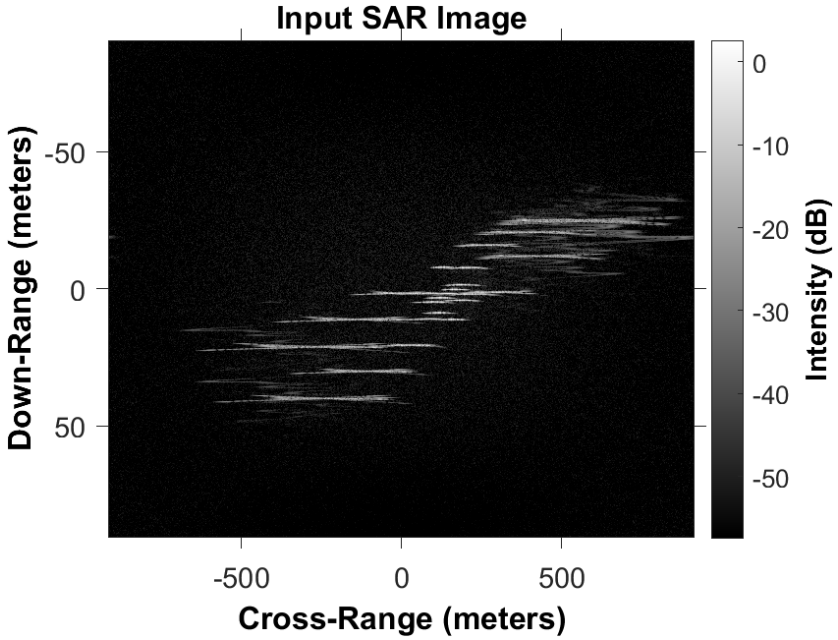

Figure 16. Default view of the target via SAR, absent from the effects of roll and pitch.

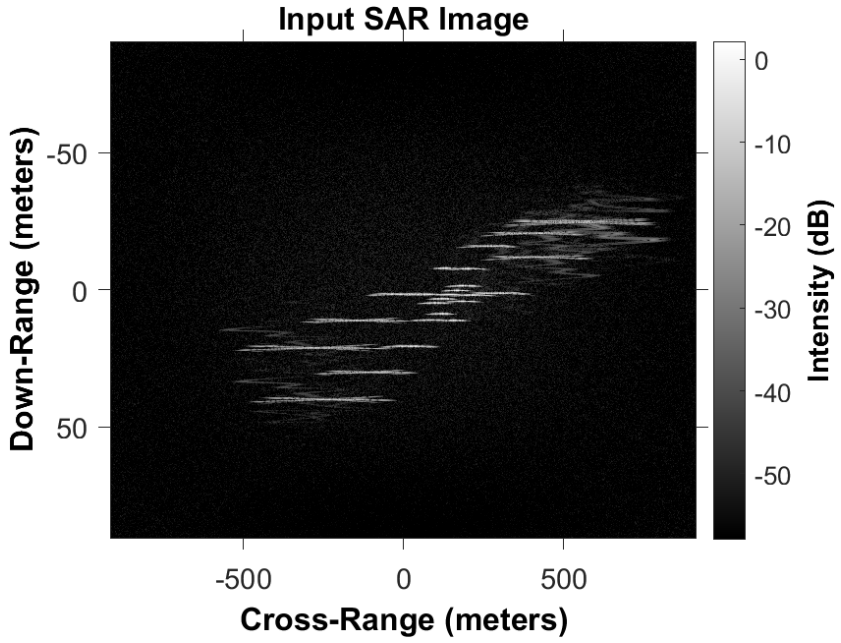

Figure 17. SAR image of target during sea state 0.

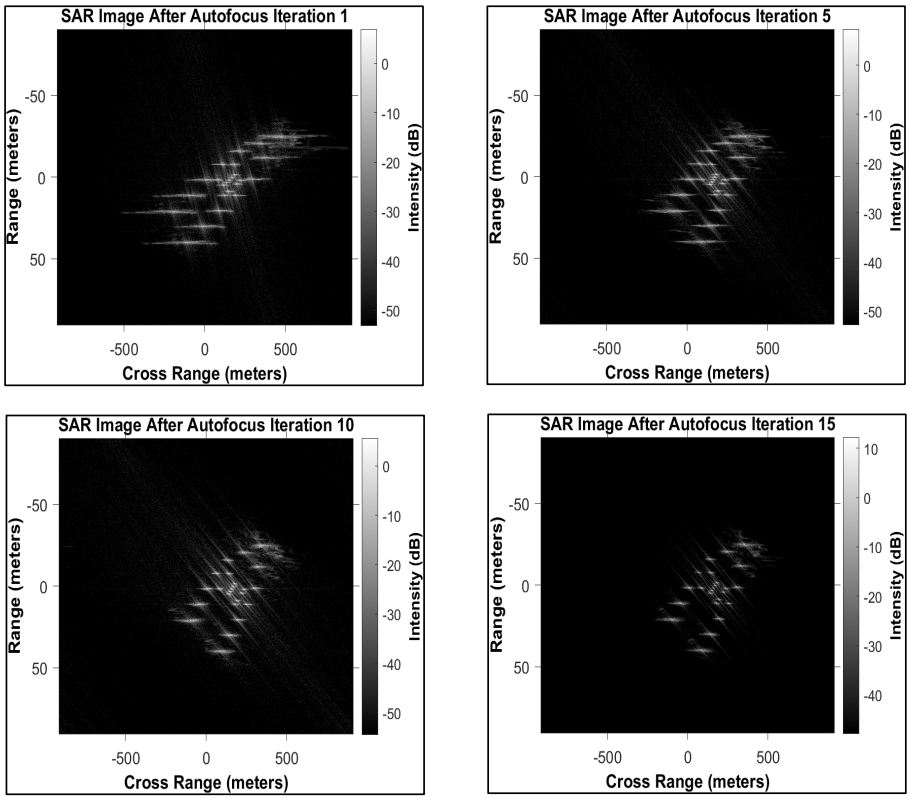

Figure 18. Sea state 0 AROMA image reformation iterations one, five, ten, and fifteen.

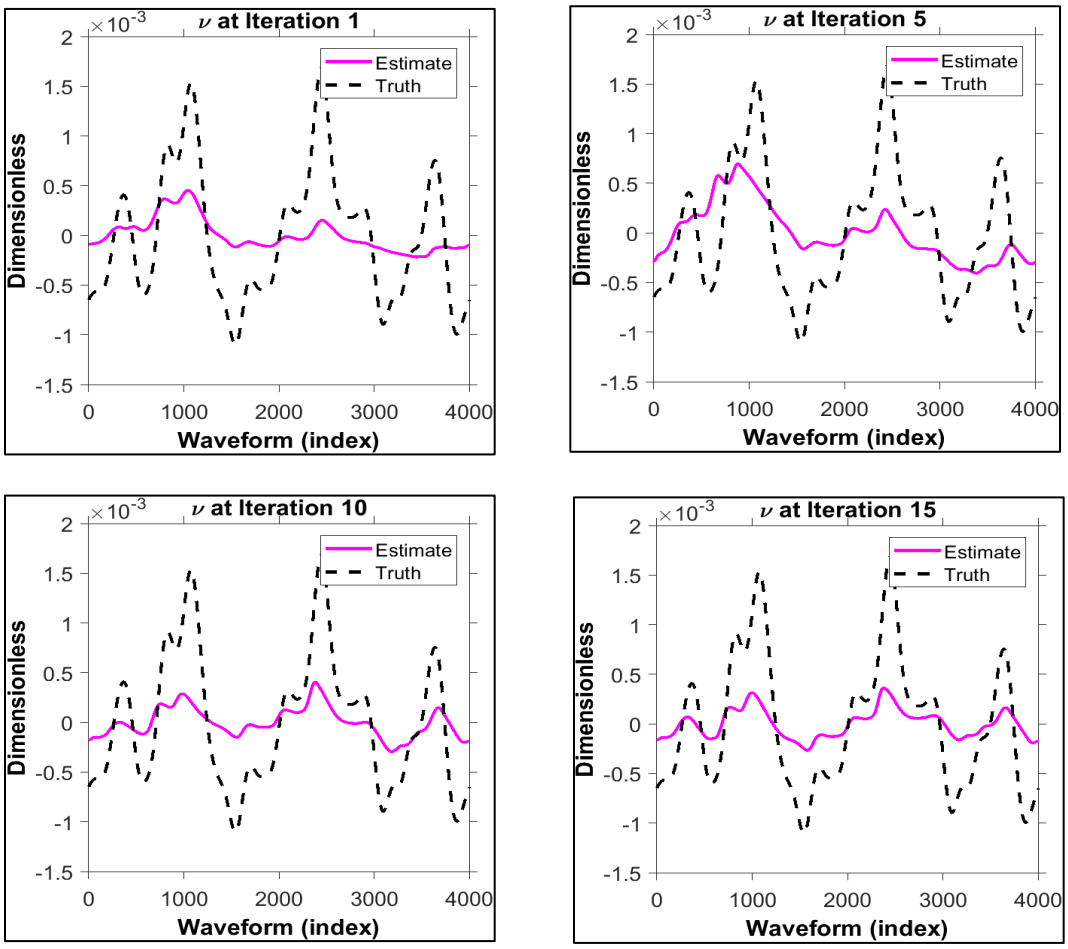

Figure 19. Sea state 0 linear phase term ν for iterations one, five, ten, and fifteen.

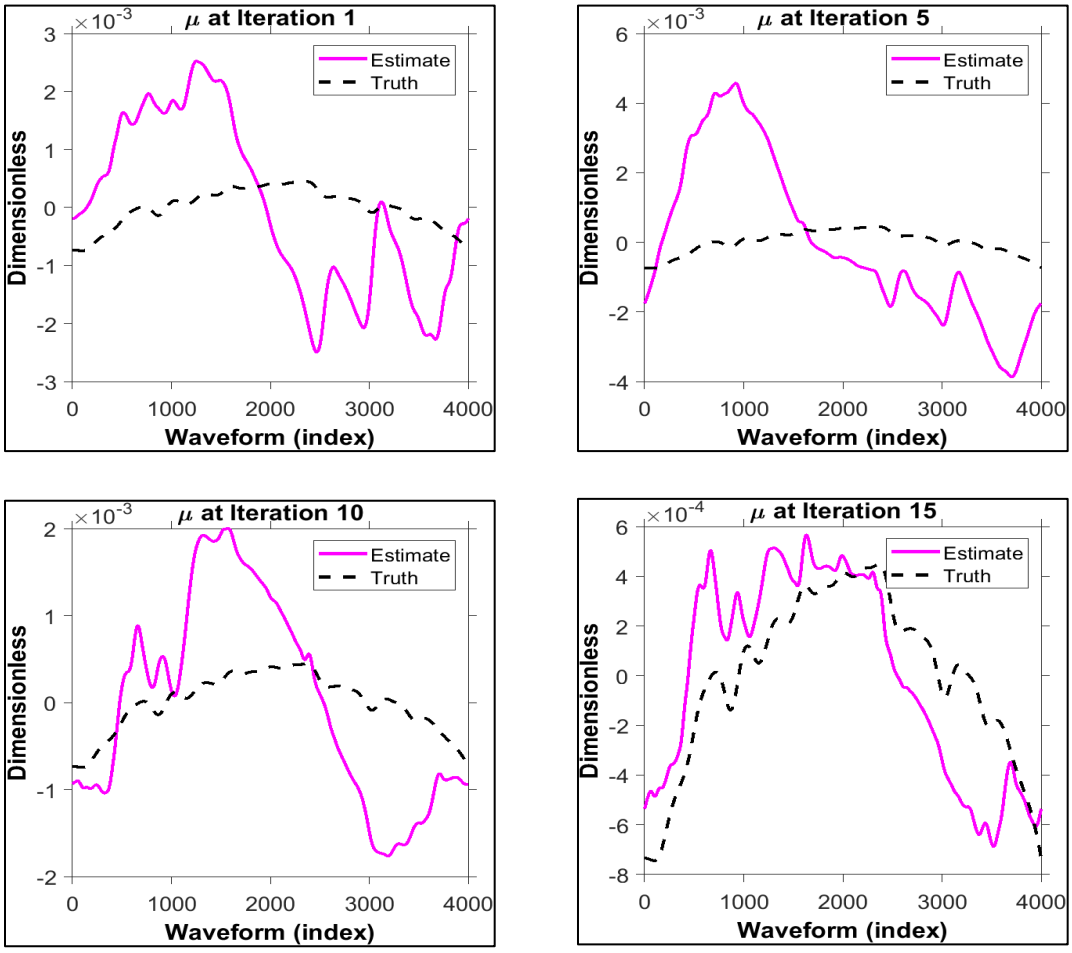

Figure 20. Sea state 0 linear phase term μ for iterations one, five, ten, and fifteen.

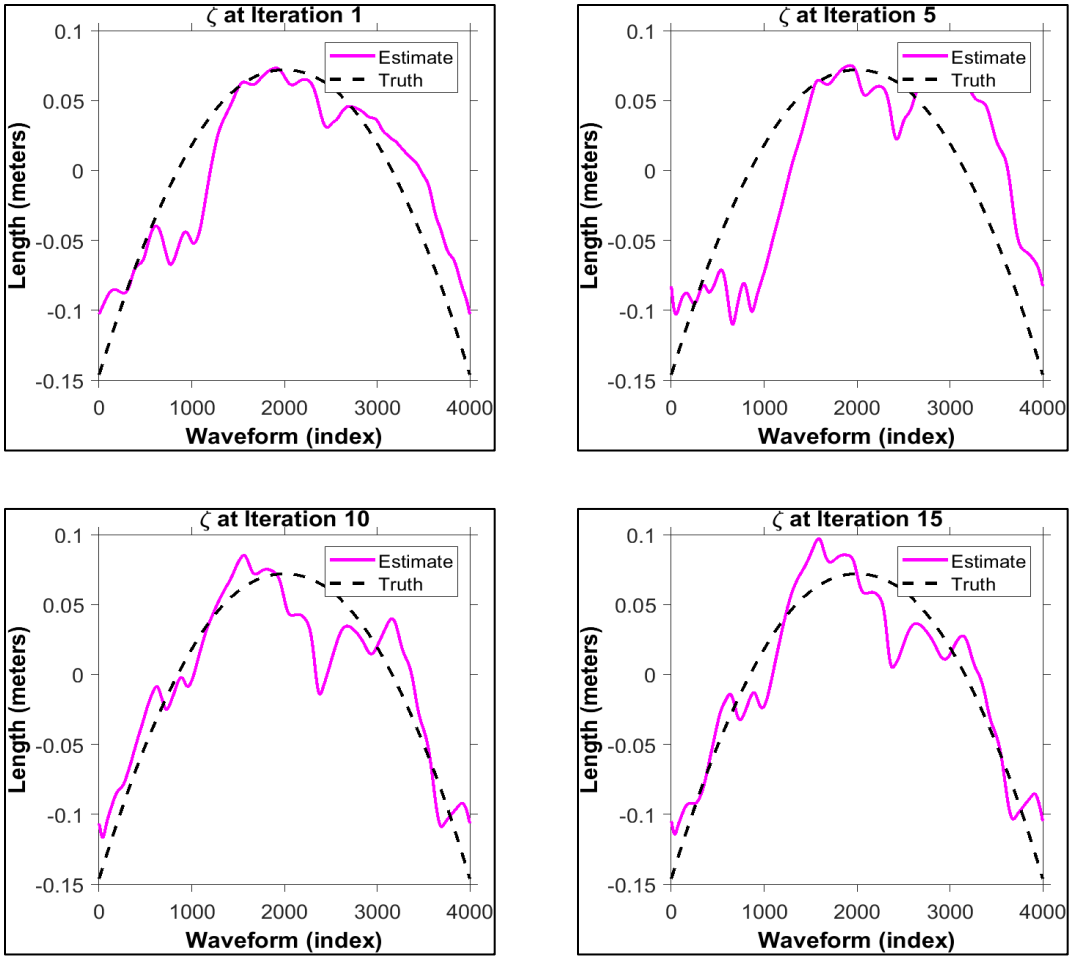

Figure 21. Sea state 0 linear phase term ζ for iterations one, five, ten, and fifteen.

B. PHASE TWO—IMAGE FORMATION SEA STATES 1 TO 4

With the introduction of pseudorandom movement that shifts the placement of the scattering centers as the roll and pitch of the target are increased, the produced images become blurred. In sea states 1 and 2, the magnitude of these angles is not enough to create a substantial amount of obscurity. At sea state 3, the motion of the scattering centers is great enough to produce noticeable and substantial smearing in the image chip. This smearing physically translates to parts of the forward and rear parts of the ship wrapping in on themselves. While not usable for operational applications that require a fine level of

precision, a cursory glance at the image would be enough to determine that there is what appears to be a ship-like structure.

Upon the application of AROMA, the SAR images produced for each sea state show an improved level of focus as is intended by the software. In sea state 1, after full image propagation and refocusing, the SAR image in Figure 25 very closely matches the image of the simulated target in Figure 13. In sea state 2, a similar outcome is observed albeit with a minimal amount of smearing in the figure. Finally, in sea state 3, the improvement from AROMA is seen most effectively. There is still a noticeable amount of smearing, the autofocus localizes the scattering centers to a point where the form of the simulated target is more readily viewed.

1. Sea State 1 Image Formation

In sea state 1, the magnitude of the roll and pitch angles is minimal as compared to sea state 0. These angles are represented in Figures 23 and 24, respectively. There is no significant change in the quality of the SAR image produced between sea states 0 and 1, with the horizontal smearing still present as observed in Figure 25. In this sea state, the overall shape of the target is still present. Figure 26 shows the result of AROMA image refocusing, where the horizontal smearing is greatly reduced. This is further evidenced in Figure 27, as iterations one, five, ten, and fifteen show the improvement between AROMA refocusing trials. The linear phase shift term ν is first represented in Figure 28, and while the estimated and true values of ν do not match perfectly, the later iterations begin to take the form of one another. Described differently, in the initial image formed the true value of the linear phase shift value is noticeably different than what the AROMA program uses for image reformation. As the AROMA program continues to sharpen the image, the simulated value of the linear phase shift approaches the true value. Figure 29 shows the linear phase shift term μ, and in the later iterations the estimation follows the true value closely. Figure 30 is the plot for the linear phase shift term ζ, and by iteration fifteen, the estimated value is very close to the true value. The iterative approach used by AROMA draws the estimated value that is used for image refocusing closer to the truth of the image, which when translated to a physical sense is the removal of the smearing in the SAR image.

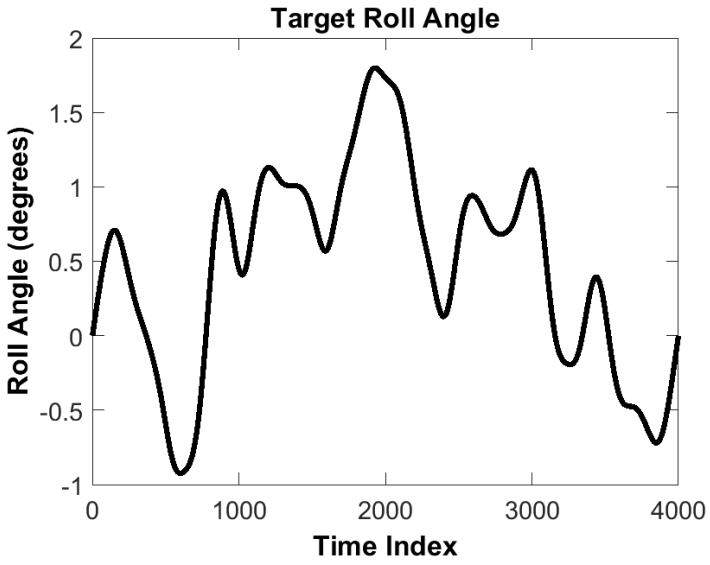

Figure 22. Target roll angle from zero to two degrees, in accordance with sea state 1 angle estimates.

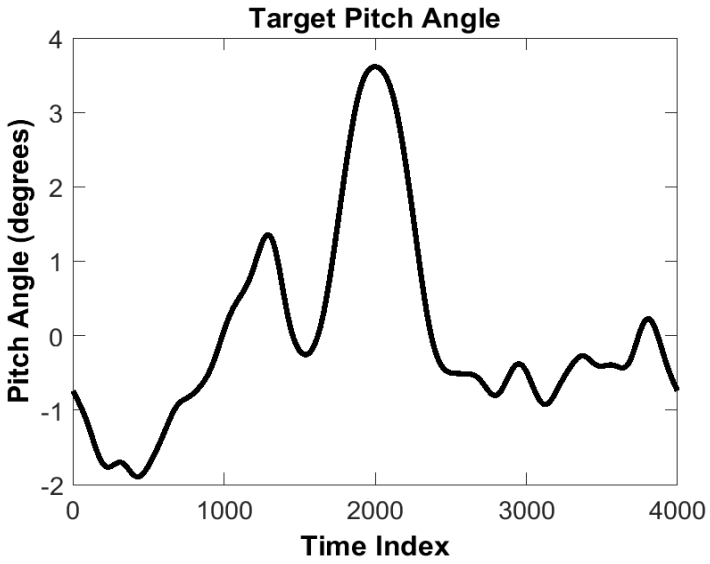

Figure 23. Target pitch angle from zero to four degrees, in accordance with sea state 1 angle estimates.

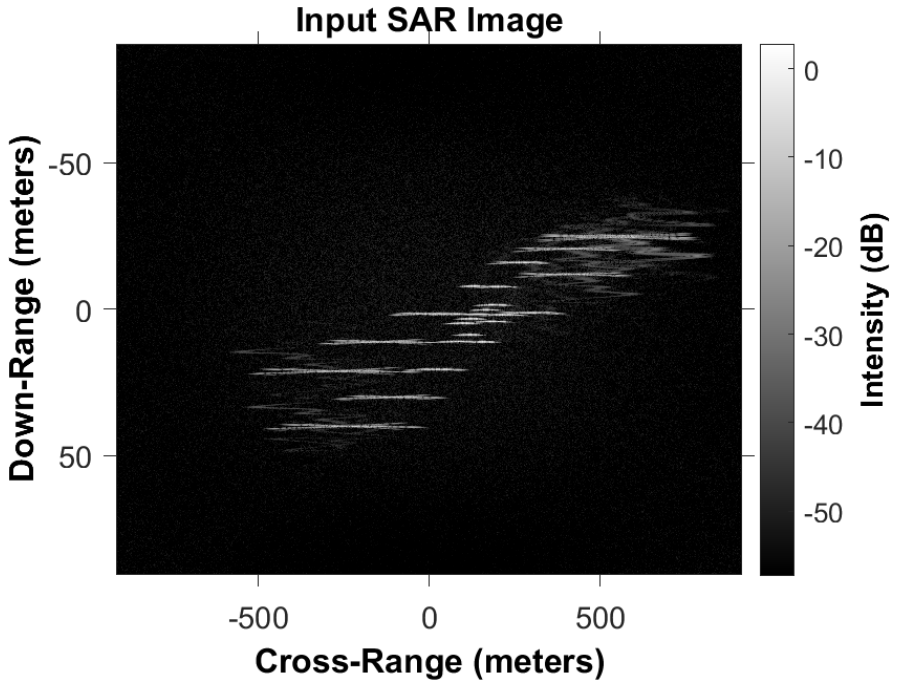

Figure 24. SAR image of simulated target during sea state 1 conditions.

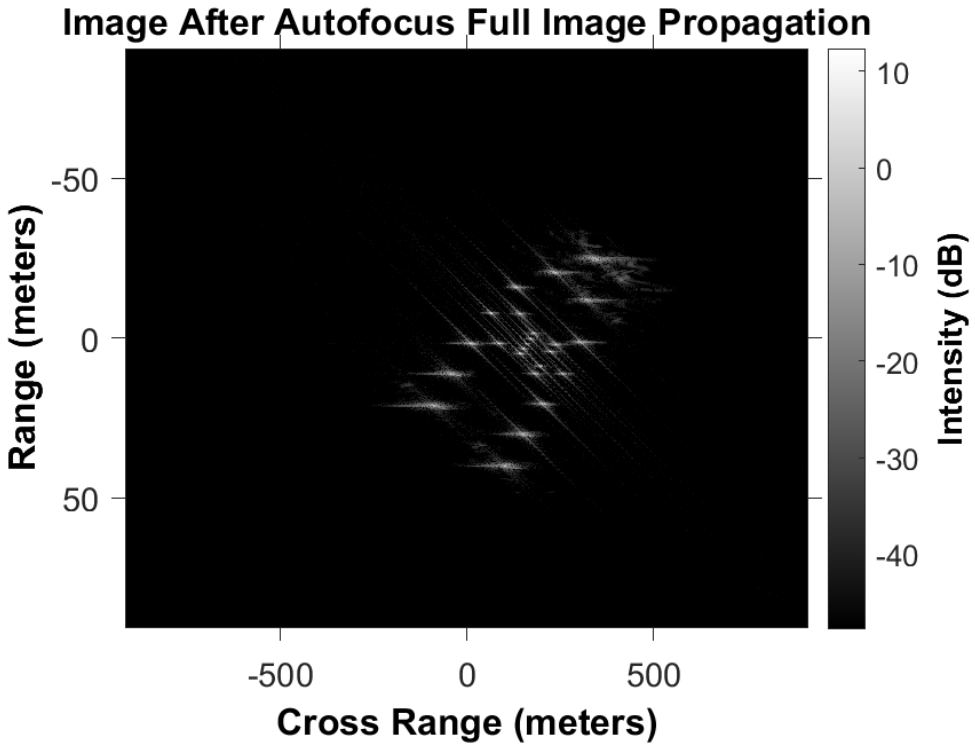

Figure 25. Sea state 1 SAR image after AROMA full image autofocus.

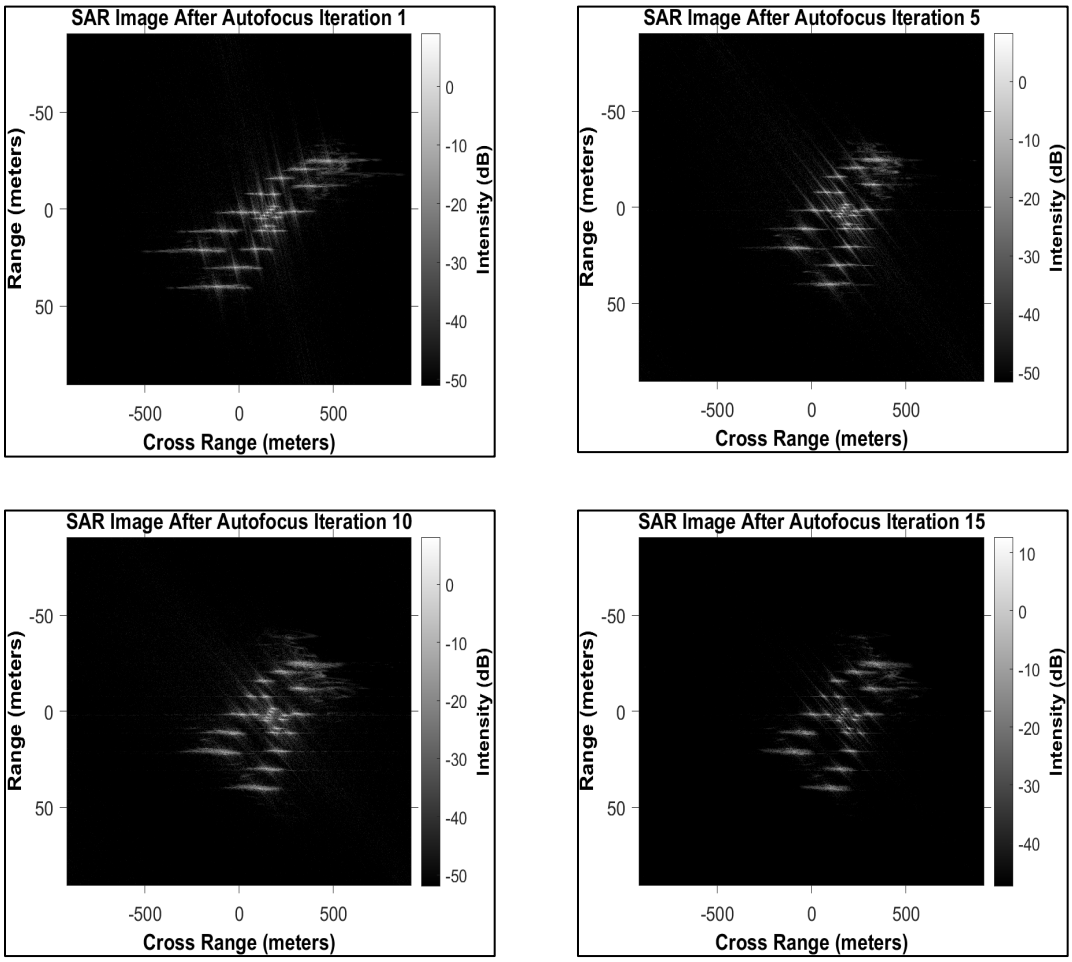

Figure 26. Sea state 1 AROMA image refocusing for iterations one, five, ten, and fifteen.

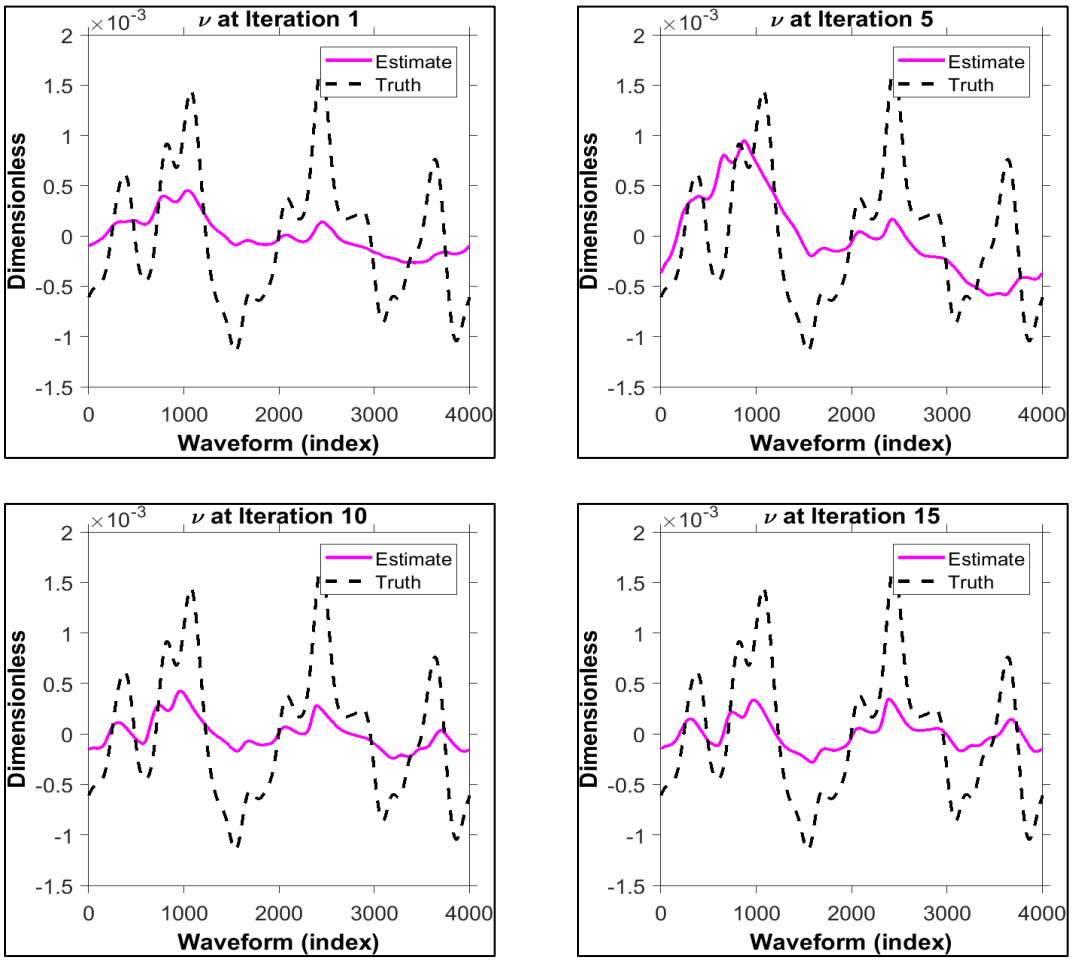

Figure 27. Sea state 1 ν AROMA refocusing for iterations one, five, ten, and fifteen.

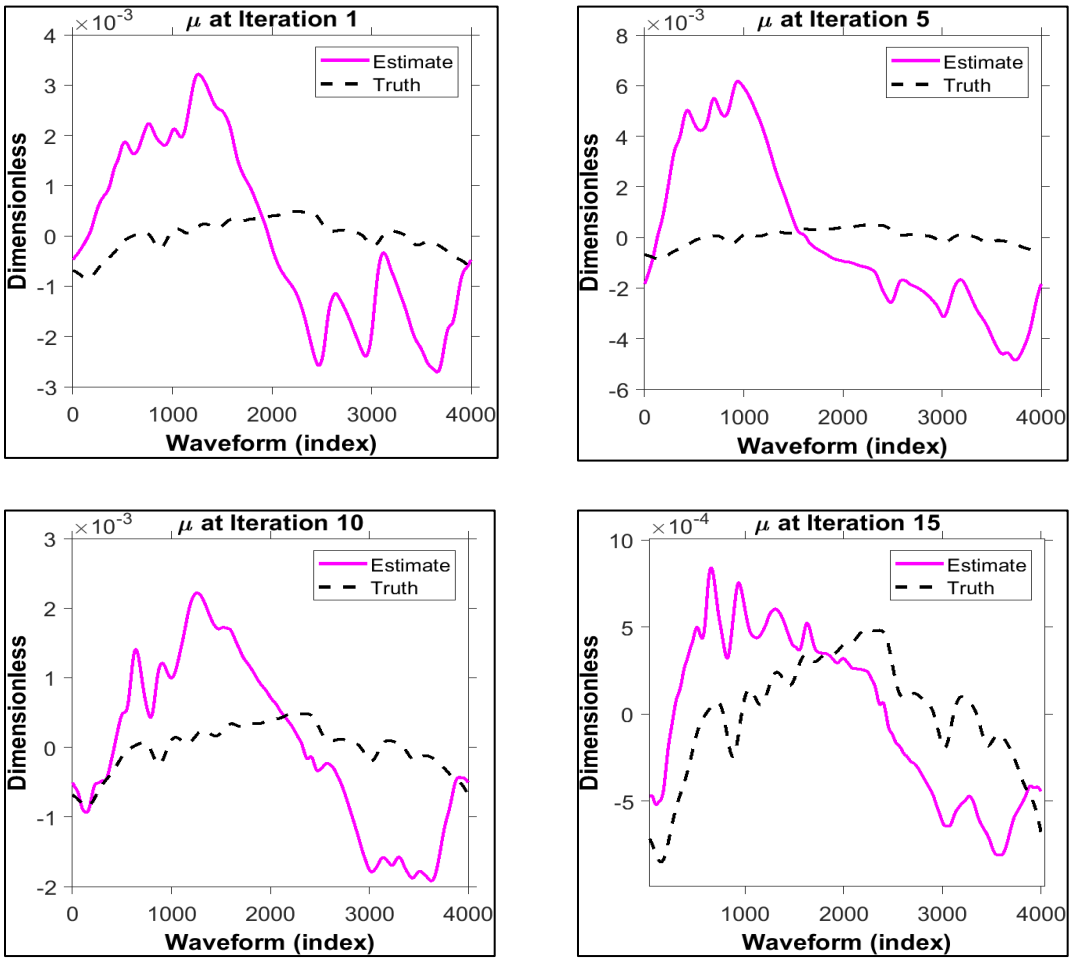

Figure 28. Sea state 1 μ AROMA refocusing for iterations one, five, ten, and fifteen.

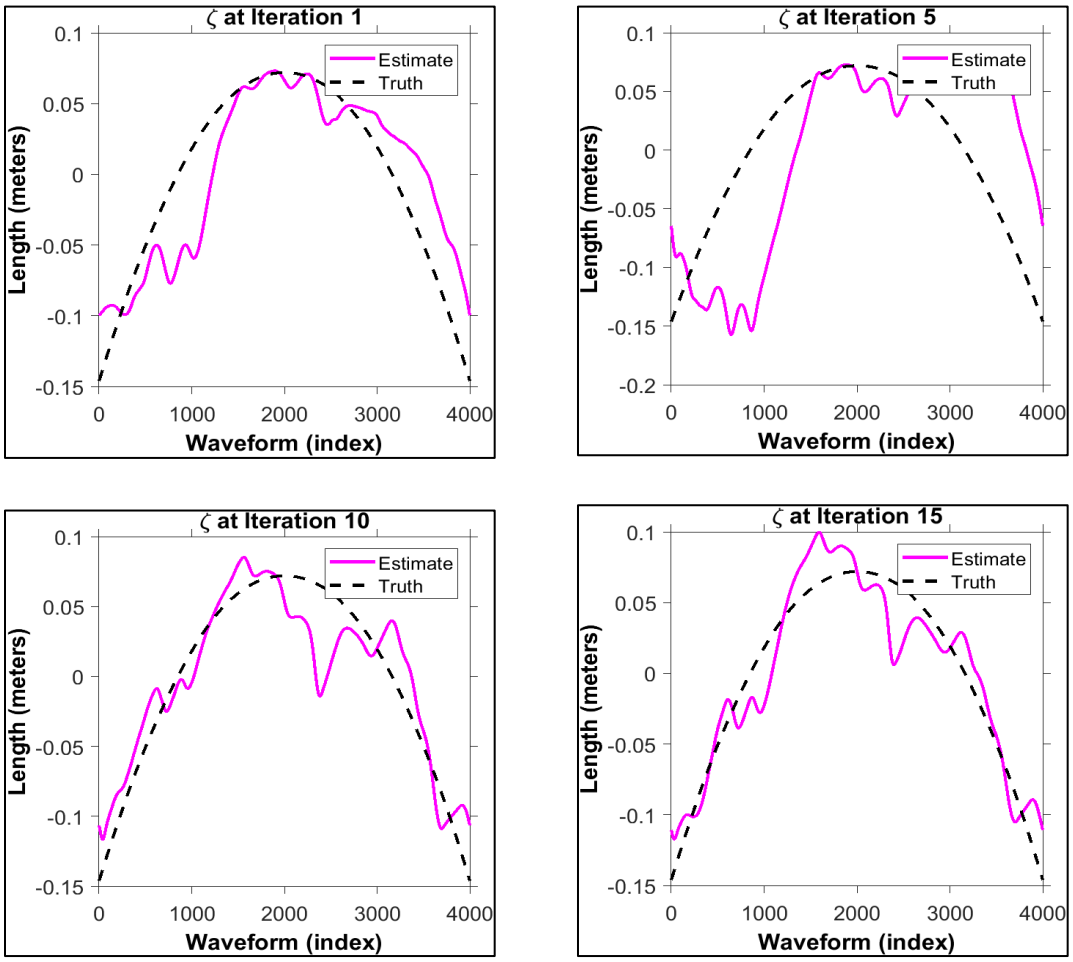

Figure 29. Sea state 1 AROMA refocusing ζ for iterations one, five, ten, and fifteen.

2. Sea State 2 Image Formation

The values of roll and pitch angles are greater at sea state 2, as evidenced in Figures 31 and 32. While there is a slight increase in smearing in the SAR image produced in Figure 33, the overall quality of the image is qualitatively like sea states 0 and 1. AROMA refocusing as depicted in Figure 34 shows a slight decrease of smearing, with the improvements shown in Figure 35 over 15 iterations of refocusing. Figures 36, 37, and 38 show the improvements of the estimated values for the linear phase shift terms like previous sea states.

Figure 30. Target roll angle from negative four to four degrees, in accordance with sea state 2 angle estimates.

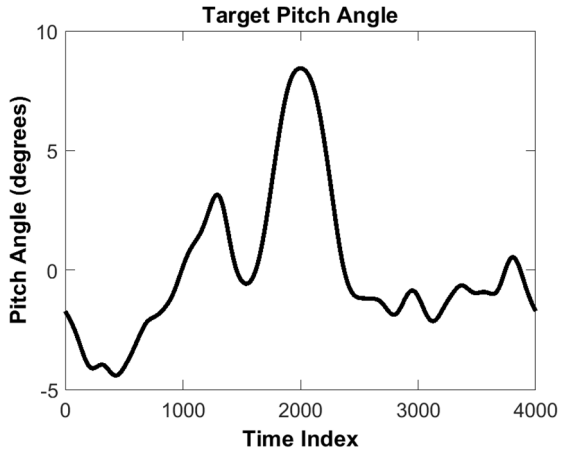

Figure 31. Target pitch angle from zero to ten degrees, in accordance with sea state 2 angle estimates.

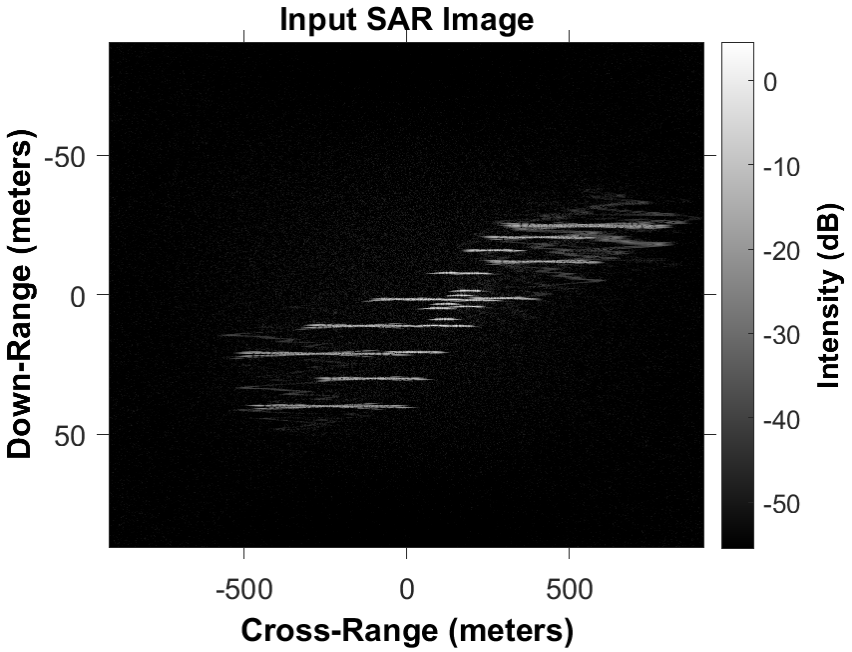

Figure 32. SAR image of simulated target during sea state 2 conditions.

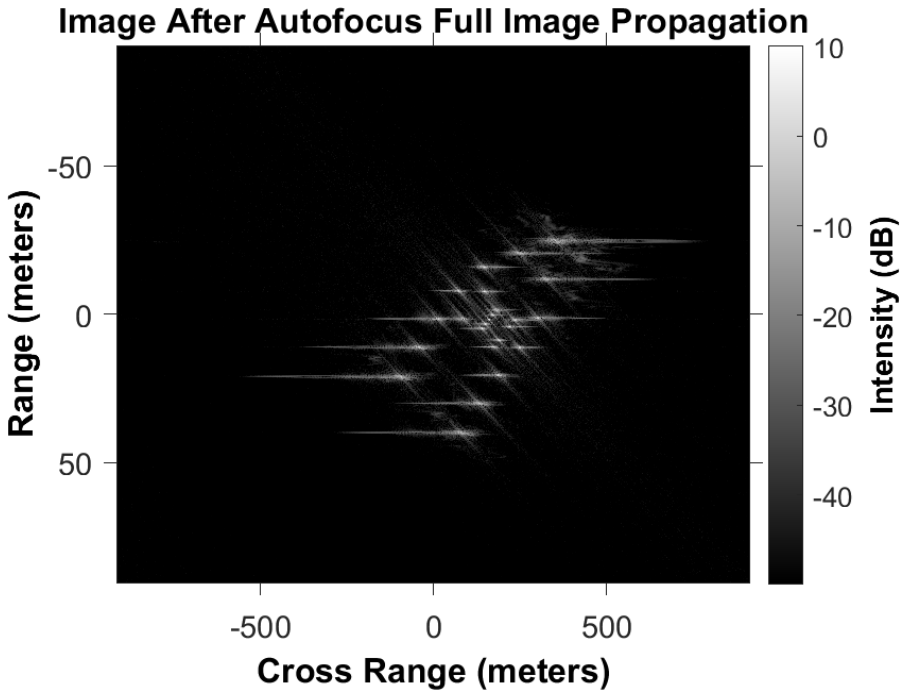

Figure 33. Sea state 2 SAR image after AROMA full image autofocus.

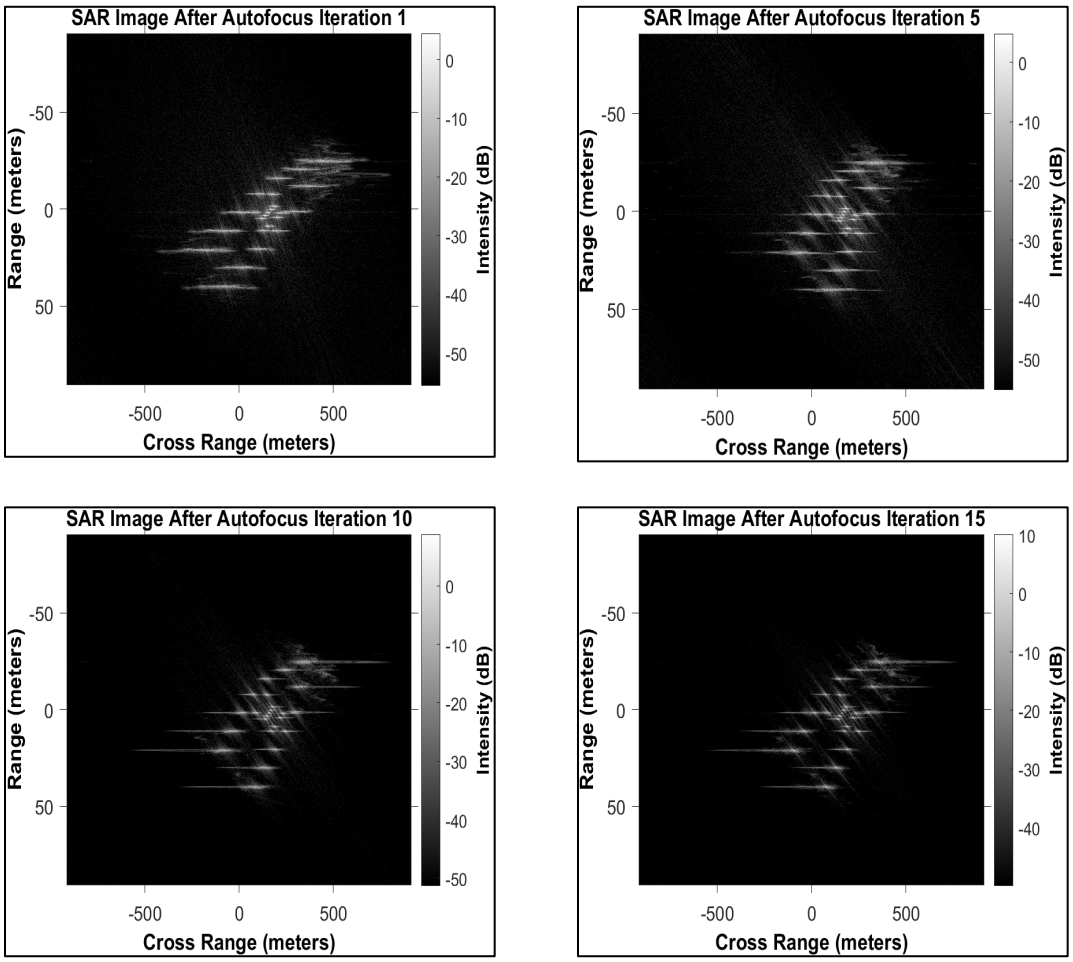

Figure 34. Sea state 2 AROMA image refocusing for iterations one, five, ten, and fifteen.

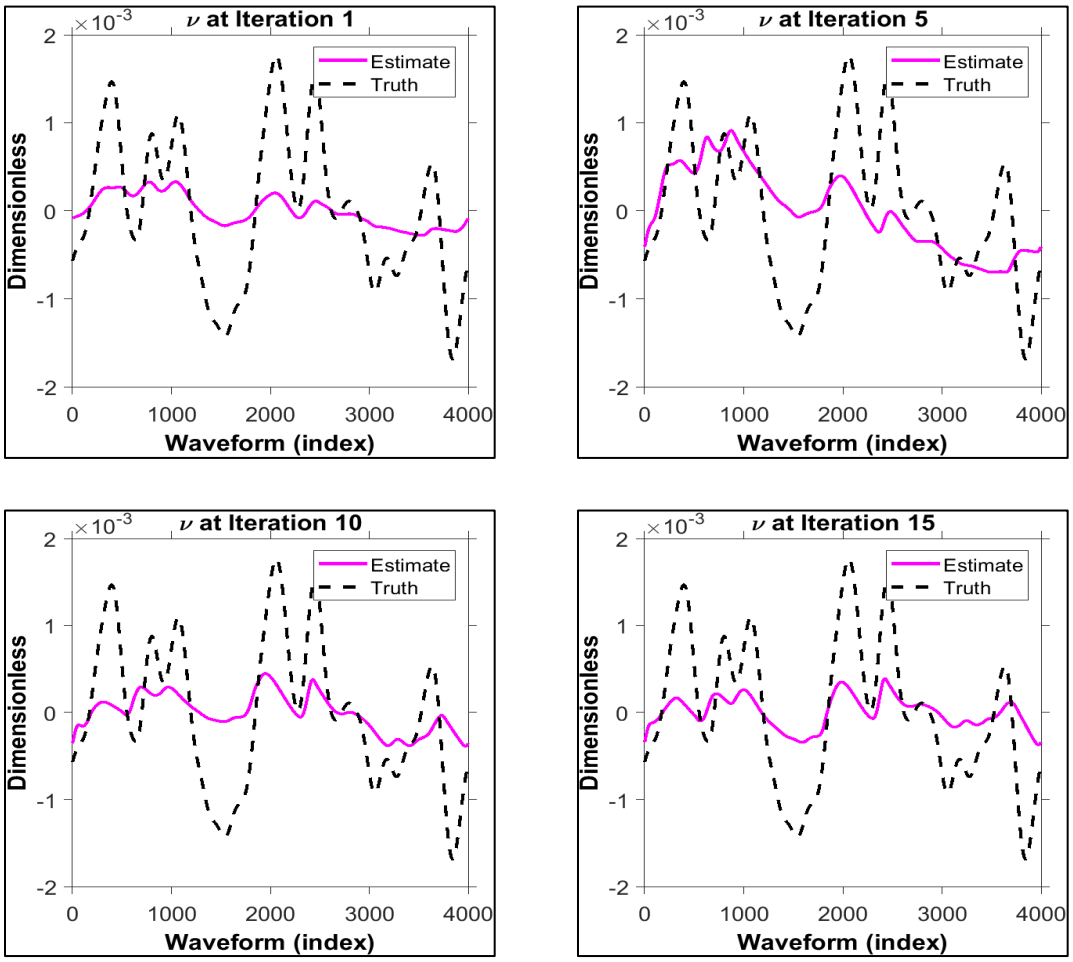

Figure 35. Sea state 2 v AROMA image refocusing iterations one, five, ten, and fifteen.

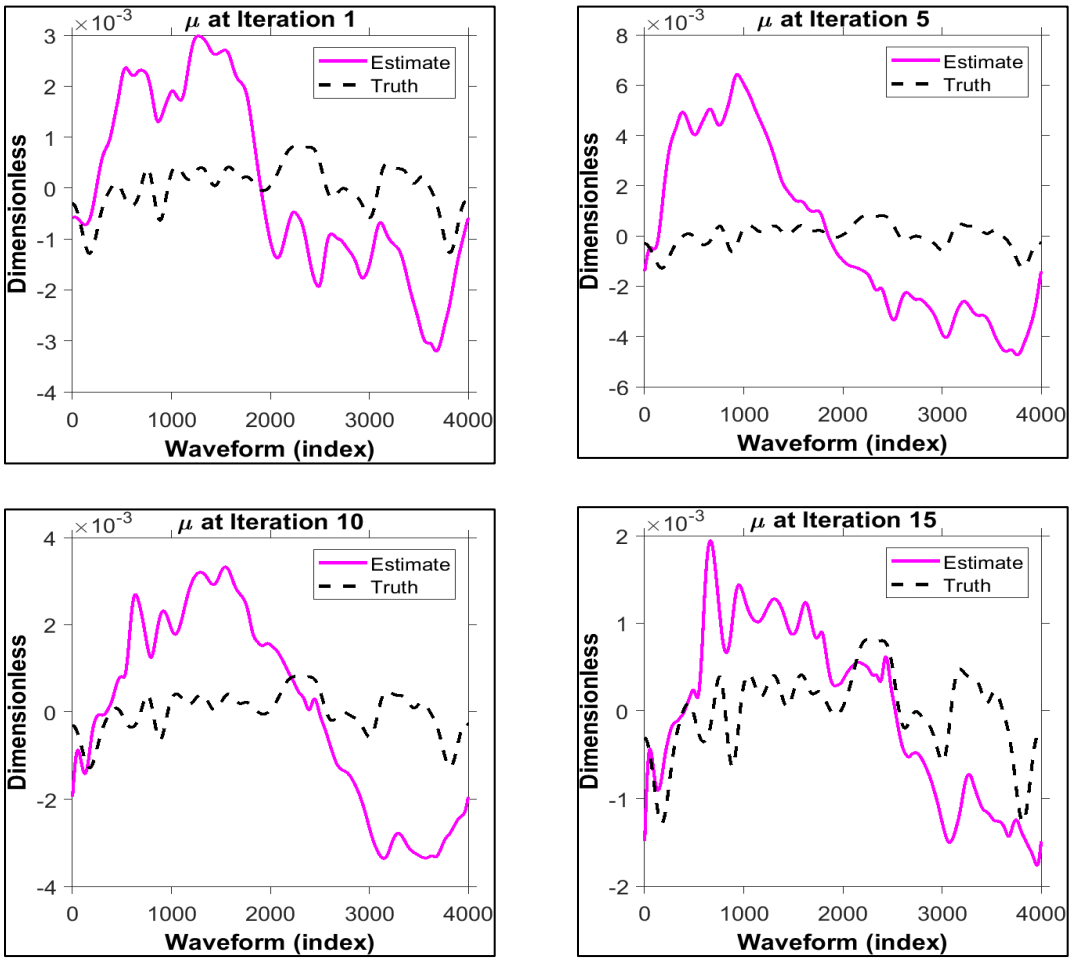

Figure 36. Sea state 2 μ AROMA image refocusing iterations one, five, ten, and fifteen.

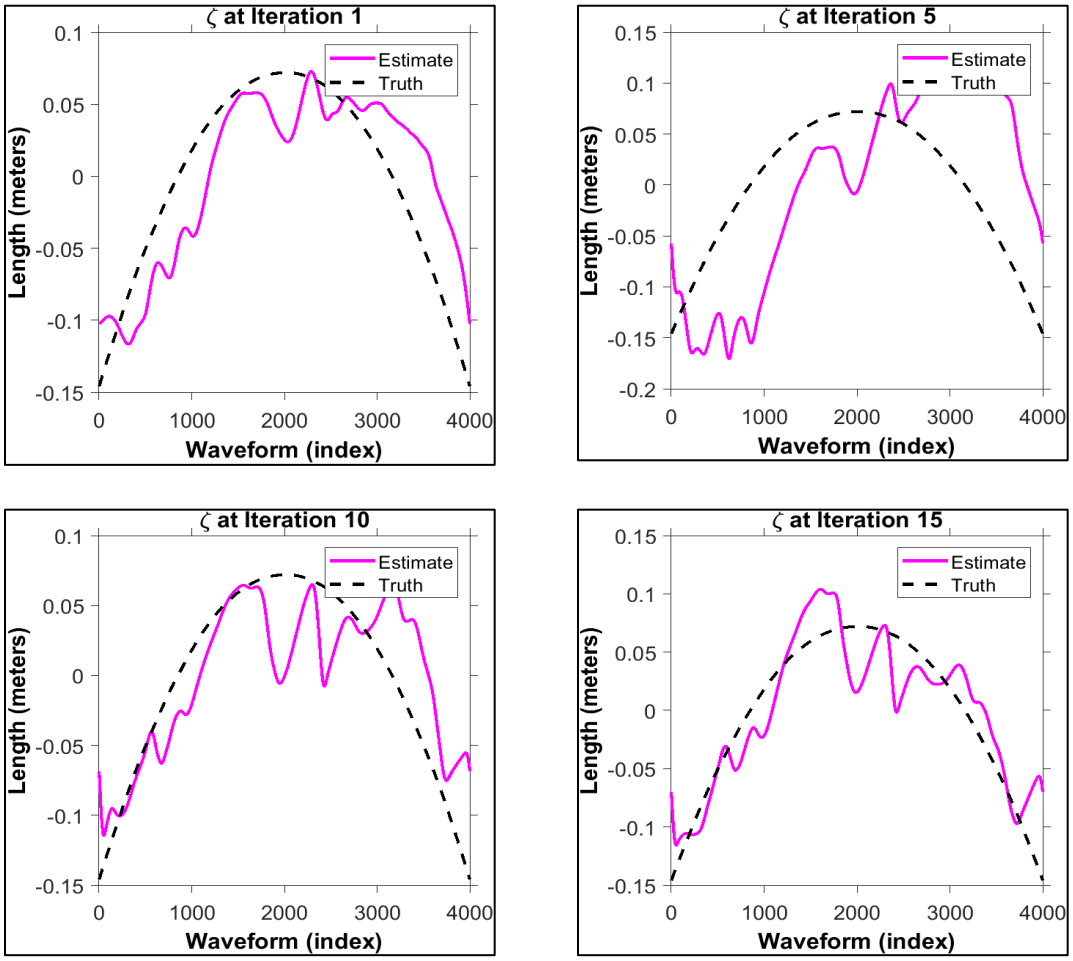

Figure 37. Sea state 2 ζ AROMA image refocusing iterations one, five, ten and fifteen.

3. Sea State 3 Image Formation

Sea State 3 is the limit of this thesis research for SAR image formation due to the common operating conditions experienced by the researcher. The roll and pitch angles are increased as shown in Figures 39 and 40, respectively. The SAR image produced in Figure 41 shows the effect that the roll and pitch have on the produced image. Due to the increased roll and pitch angles, heavy smearing occurs as the scattering centers are disturbed. Of note, there is a slight aliasing effect observed in Figure 41, which when translated physically can be considered as edges of the simulated target wrapping upon each other. In Figure 42, AROMA refocusing is represented, and while smearing still exists, the brightness of the scattering centers in the middle of these smears matches relatively closely to the original position of the scattering centers. From a qualitative perspective, it is possible to discern the broad shape of the simulated target out of the smears, which constitutes a successful use of AROMA to refocus a simulated maritime target. However, the quality of this refocusing is not enough to provide a clear view of the estimated target. Further refinement of this process may prove fruitful, as well as the inclusion of more scattering centers. The improvement over 15 iterations of image refocusing is represented by Figure 43, and the drop off in horizontal smearing is substantial. Figures 44, 45, and 46 show the estimated vs. true values of the linear phase shift terms, and of note there are still vast differences between the estimated and true values of these terms in each respective iteration. These differences are directly related to the smearing seen in the refocused SAR image of Figure 42.

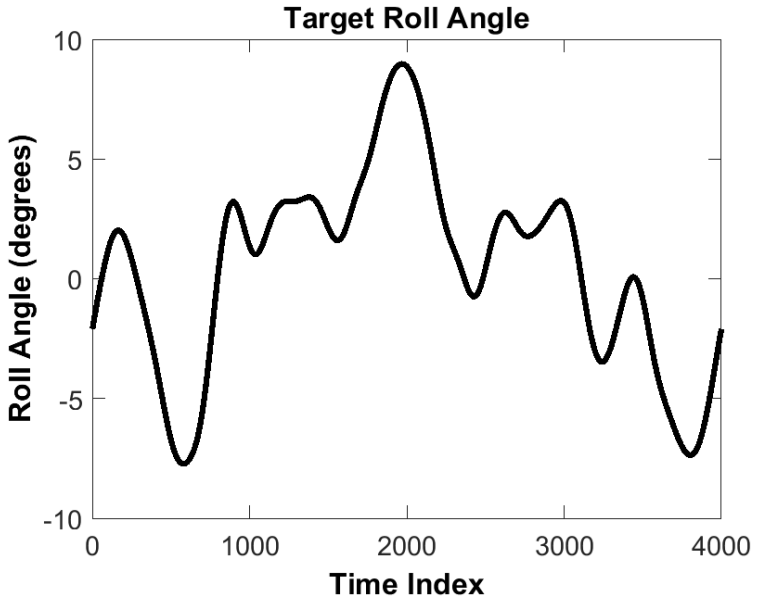

Figure 38. Target roll angle from zero to ten degrees, in accordance with sea state 3 angle estimates

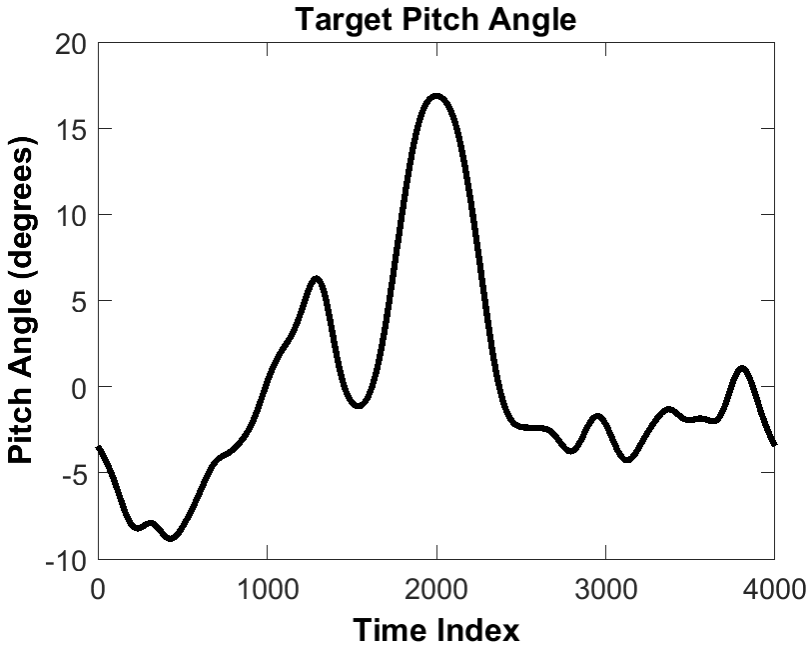

Figure 39. Target pitch angle from zero to twenty degrees, in accordance with sea state 3 angle estimates

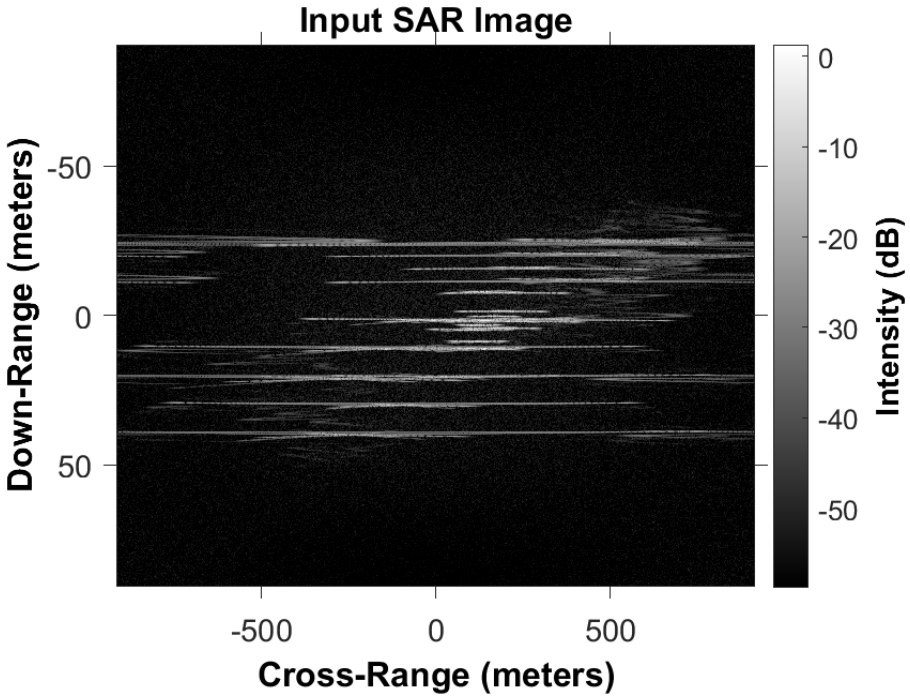

Figure 40. SAR image of simulated target during sea state 3 conditions.

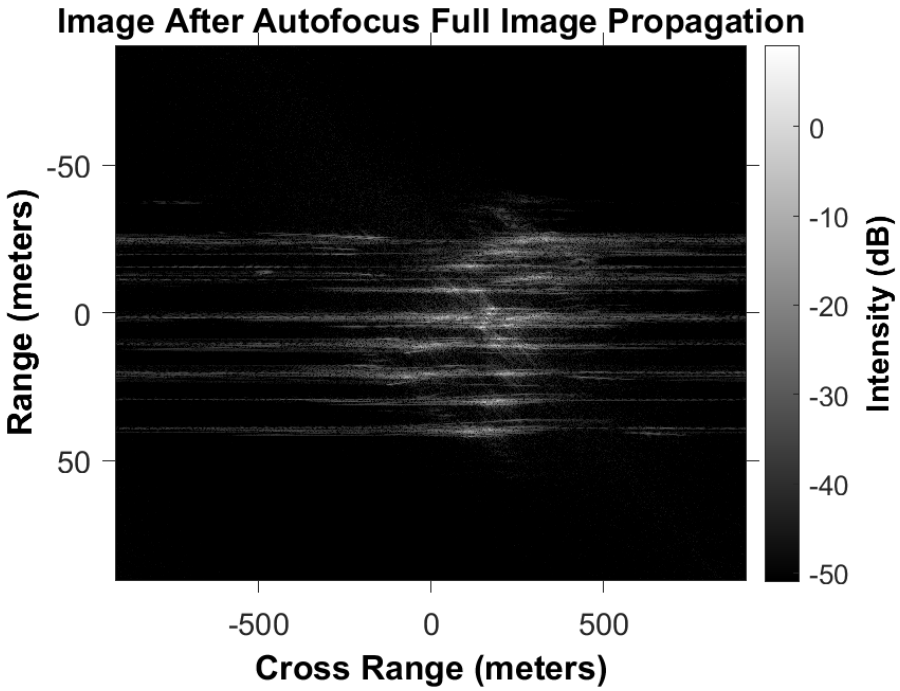

Figure 41. Sea state 3 SAR image after AROMA full image autofocus.

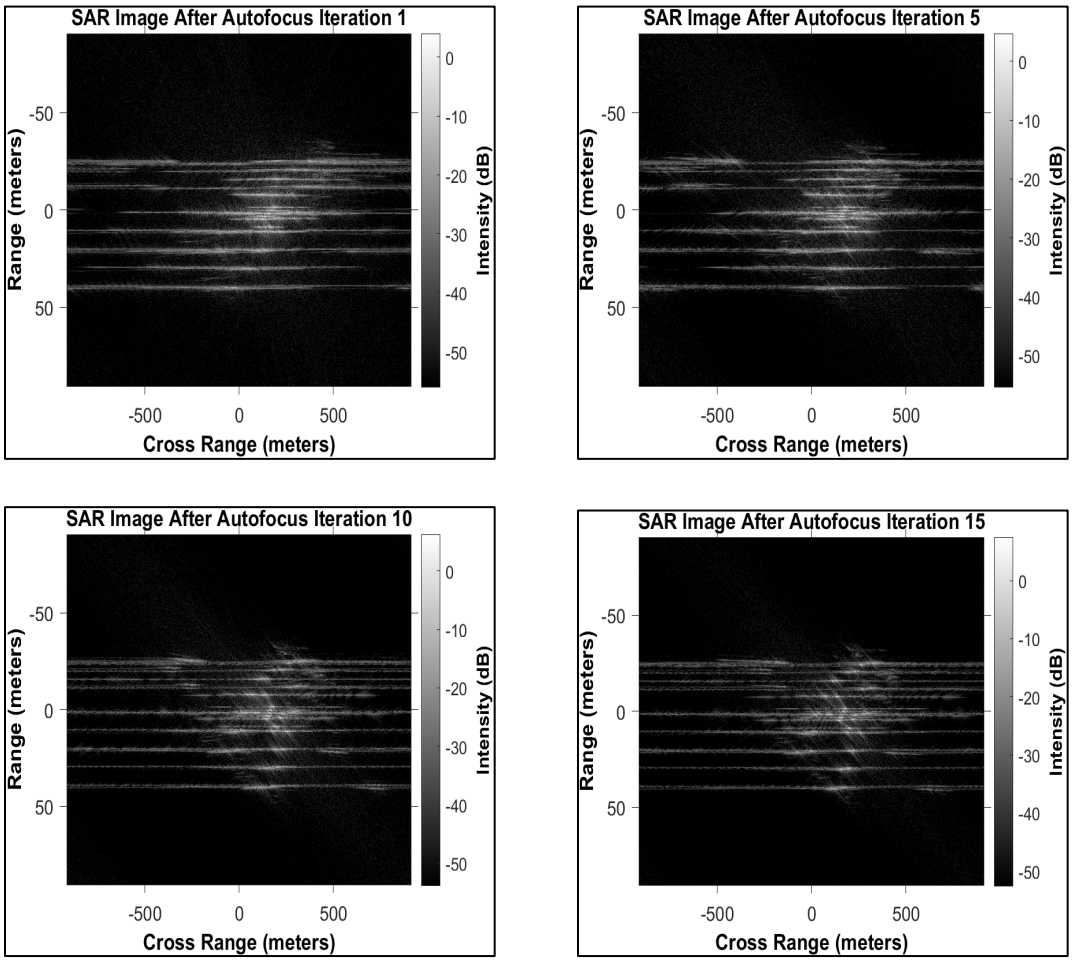

Figure 42. Sea state 3 AROMA image reformation for iterations one, five, ten, and fifteen.

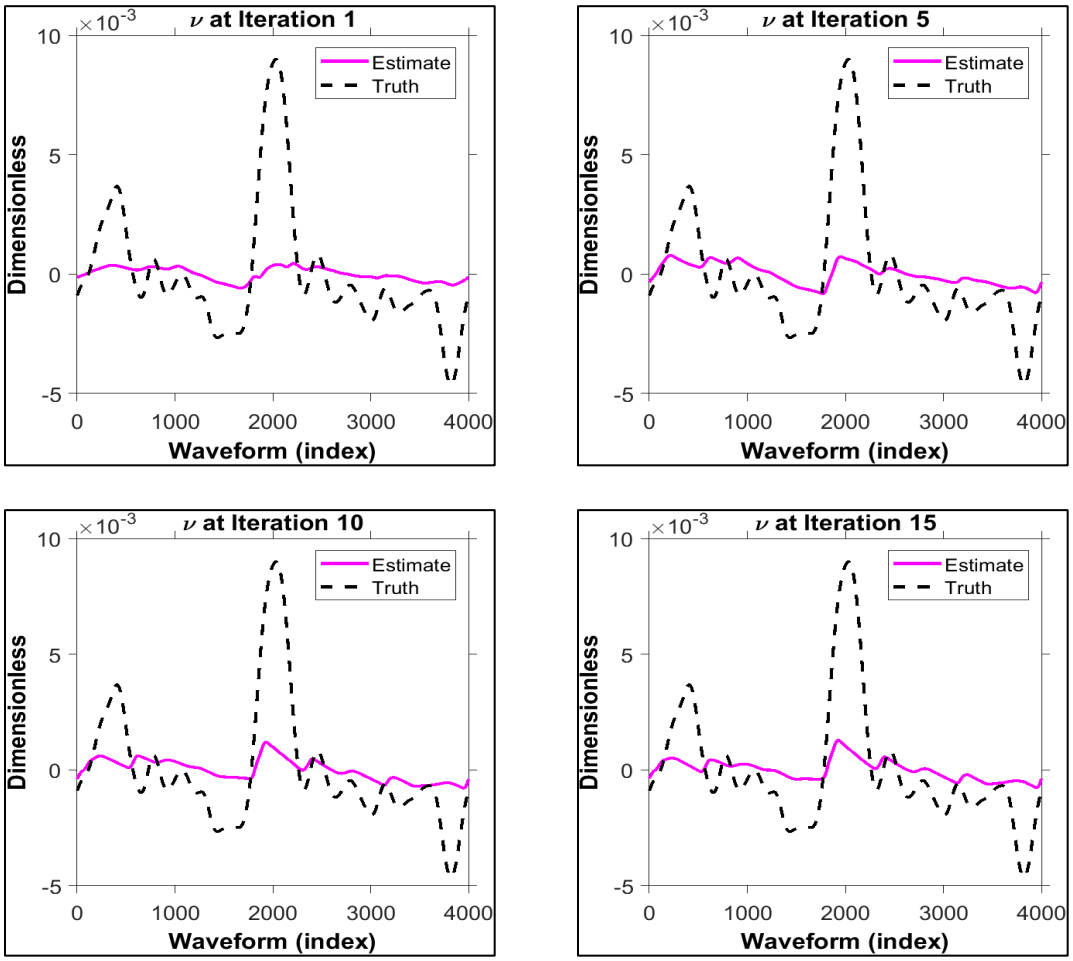

Figure 43. Sea state 3 ν AROMA image reformation for iterations one, five, ten, and fifteen.

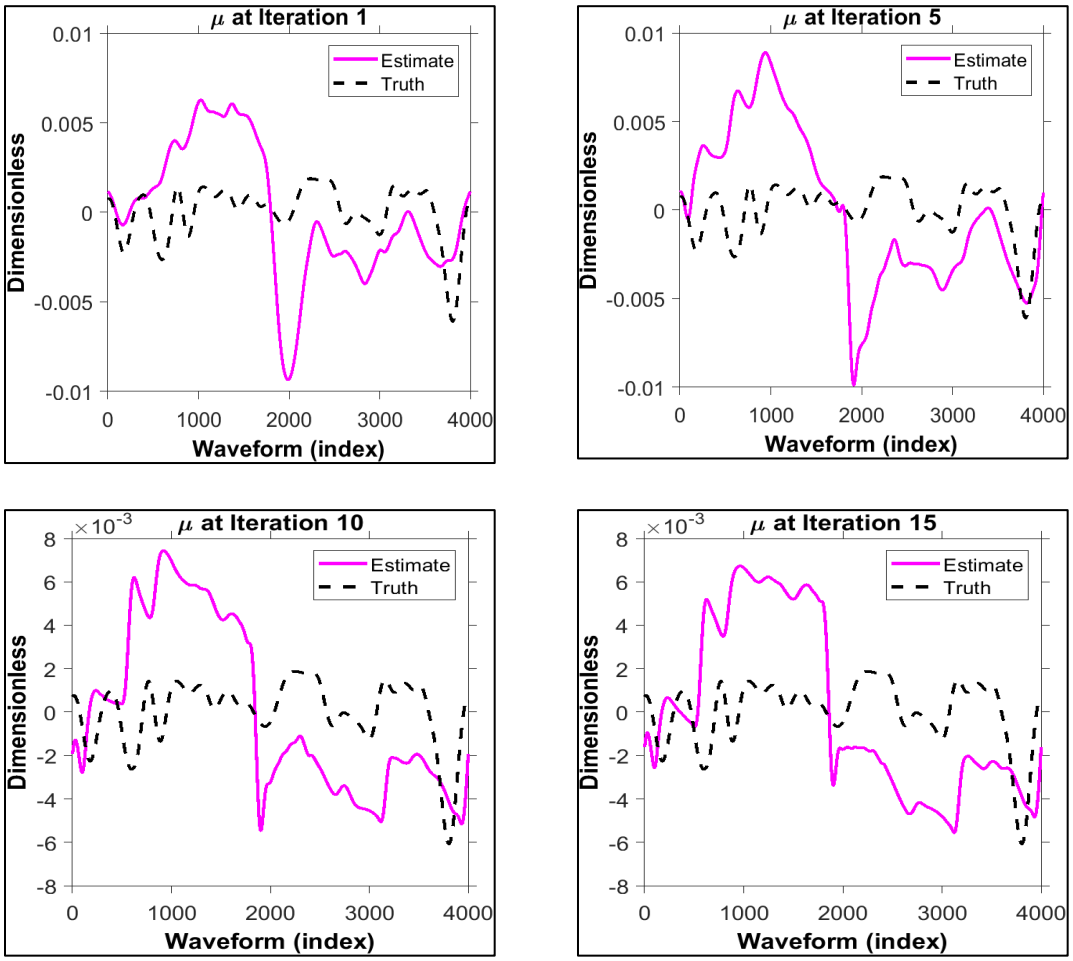

Figure 44. Sea state 3 μ AROMA image reformation for iterations one, five, ten, and fifteen.

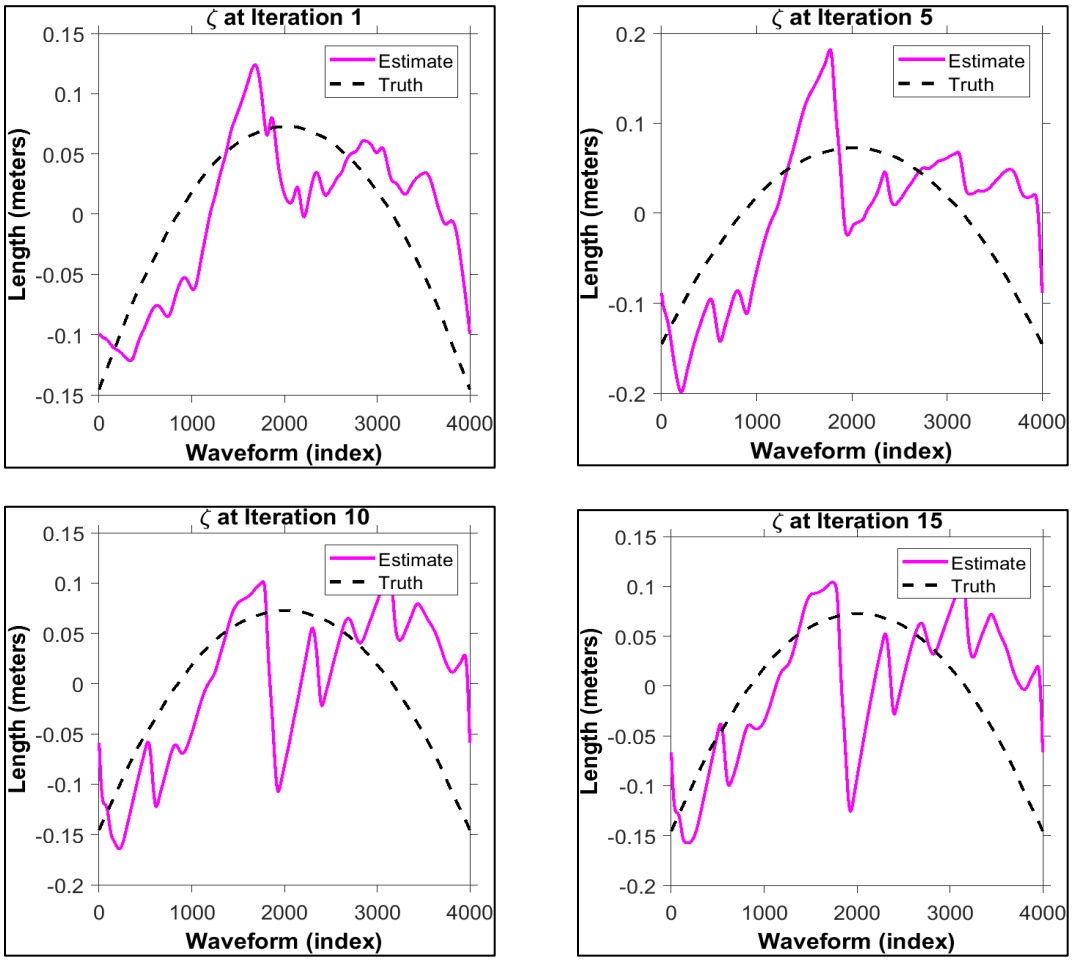

Figure 45. Sea state 3 ζ AROMA image reformation for iterations one, five, ten, and fifteen.

THIS PAGE INTENTIONALLY LEFT BLANK

V. CONCLUSION AND FUTURE WORK

This thesis investigated the hypothesis of whether readily available operational radar parameters have merit for the possibility of producing high fidelity imagery local to a surface combatant. Using MATLAB code, a data-driven solution is developed in support of the validity of the idea of a SAR being used for imagery purposes for service on-board U.S. maritime vessels. This would make it possible to provide higher fidelity imagery to decision makers and warfighters, provided appropriate conditions for design are implemented, to provide as much information to the surface combatant as quickly as possible and under the control of these individuals. The benefit of this system being developed is the decrease in time between detection and engagement in the DTE sequence, and more rapid positive identification of threats. There are several topics within this thesis that can be explored in future work to expand on the potential capability as discussed in the previous chapters. Increased complexity with the simulation of roll, pitch, and yaw could prove fruitful with increased fidelity in near real-world conditions. Additionally, changes in propagation characteristics of the intended sensor should be experimented on to increase the quality of images, as well as extend the possible range of the sensor. Finally, upon successful computer simulation, a hardware build would prove fruitful in bringing the concept of organic maritime SAR/ISAR imaging capability to reality.

THIS PAGE INTENTIONALLY LEFT BLANK

LIST OF REFERENCES

[1] J. Lu, *Design Technology of Synthetic Aperture Radar.* Hoboken, NJ, USA: John Wiley & Sons, 2019 [Online]. Available: Wiley Online Library.

[2] M. Richards, J. Scheer, and W. Holm, Eds., *Principles of Modern Radar* Volume 1. Raleigh, NC, USA: SciTech Publishing, 2015.

[3] R. S. Howard and H. D. Vaughan, *Navy Electricity and Electronics Training Series Module 10: Introduction to Wave Propagation, Transmission Lines, and Antennas*. Pensacola, FL, USA: Naval Education and Training Professional Development and Technology Center, 1998.

[4] "Range Resolving techniques," class notes for EC4615 Advanced RADAR, Dept. of Electronic and Computer Engineering, Naval Postgraduate School, Monterey, CA, USA, fall 2021.

[5] V. Chen and M. Martorella, *Inverse Synthetic Aperture Radar Imaging: Principles, Algorithms and Applications.* Raleigh, NC, USA: SciTech Publishing, 2014.

[6] N. Friedman, *The Naval Institute Guide to World Naval Weapon Systems.* Annapolis, MD, USA: Naval Institute Press, 2006

[7] Furuno Electronic Co. *Furuno Operator's Manual, Marine radar Model 1937*, Nishinomiya, Japan, 2009 [Online]. Available: https://www.furuno.com/files/Manual/37/upload/OME35820D1_MODEL1937.pdf

[8] D. A. Garren, "Theory of arbitrary rigid object motion autofocus for non-uniform target rotation and translation*," IET radar, Sonar & Navigation*, vol. 14, no. 11, pp. 1803–1814, 2020.

[9] C. V. Jakowatz Jr., D. E. Wahl, and P. H. Eichel, "Refocus of constant velocity moving targets in synthetic aperture radar imagery" in *1998 Proc. SPIE: Algorithms for Synthetic Aperture Radar Imagery V Conf.*, Orlando, FL, USA, 13–17 April 1998.

[10] J C. V. Jakowatz Jr., D. E. Wahl, and P. H. Eichel, *Spotlight-Mode Synthetic Aperture RADAR: A signal Processing Approach*. Berlin, Germany: Sandia National Laboratories, Springer Science Business and Media, 1996, pp. 221–271

[11] Exploring Our Fluid Earth Team, University of Hawaii Manoa, “Sea states,” Accessed May 2, 2023 [Online] Available https://manoa.hawaii.edu/exploringourfluidearth/physical/waves/sea-states

[12] Doerry, A. W., “Ship Dynamics for Maritime ISAR Imaging.” Livermore, CA, USA: Sandia National Laboratories, SAND2008-1020, 2008 [Online] Available: https://www.osti.gov/servlets/purl/929523

INITIAL DISTRIBUTION LIST

1. Defense Technical Information Center
   Ft. Belvoir, Virginia

2. Dudley Knox Library
   Naval Postgraduate School
   Monterey, California